NUREG/CR-6422
BNL-NUREG-52491

Power Excursion Analysis for High Burnup Cores

Prepared by
D. J. Diamond, L. Neymotin, P. Kohut

Brookhaven National Laboratory

Prepared for
U.S. Nuclear Regulatory Commission

AVAILABILITY NOTICE

Availability of Reference Materials Cited in NRC Publications

Most documents cited in NRC publications will be available from one of the following sources:

1. The NRC Public Document Room, 2120 L Street, NW., Lower Level, Washington, DC 20555-0001

2. The Superintendent of Documents, U.S. Government Printing Office, P. O. Box 37082, Washington, DC 20402-9328

3. The National Technical Information Service, Springfield, VA 22161-0002

Although the listing that follows represents the majority of documents cited in NRC publications, it is not intended to be exhaustive.

Referenced documents available for inspection and copying for a fee from the NRC Public Document Room include NRC correspondence and internal NRC memoranda; NRC bulletins, circulars, information notices, inspection and investigation notices; licensee event reports; vendor reports and correspondence; Commission papers; and applicant and licensee documents and correspondence.

The following documents in the NUREG series are available for purchase from the Government Printing Office: formal NRC staff and contractor reports, NRC-sponsored conference proceedings, international agreement reports, grantee reports, and NRC booklets and brochures. Also available are regulatory guides, NRC regulations in the *Code of Federal Regulations*, and *Nuclear Regulatory Commission Issuances*.

Documents available from the National Technical Information Service include NUREG-series reports and technical reports prepared by other Federal agencies and reports prepared by the Atomic Energy Commission, forerunner agency to the Nuclear Regulatory Commission.

Documents available from public and special technical libraries include all open literature items, such as books, journal articles, and transactions. *Federal Register* notices, Federal and State legislation, and congressional reports can usually be obtained from these libraries.

Documents such as theses, dissertations, foreign reports and translations, and non-NRC conference proceedings are available for purchase from the organization sponsoring the publication cited.

Single copies of NRC draft reports are available free, to the extent of supply, upon written request to the Office of Administration, Distribution and Mail Services Section, U.S. Nuclear Regulatory Commission, Washington, DC 20555-0001.

Copies of industry codes and standards used in a substantive manner in the NRC regulatory process are maintained at the NRC Library, Two White Flint North, 11545 Rockville Pike, Rockville, MD 20852-2738, for use by the public. Codes and standards are usually copyrighted and may be purchased from the originating organization or, if they are American National Standards, from the American National Standards Institute, 1430 Broadway, New York, NY 10018-3308.

DISCLAIMER NOTICE

NUREG/CR-6422
BNL-NUREG-52491

Power Excursion Analysis for High Burnup Cores

Manuscript Completed: December 1995
Date Published: February 1996

Prepared by
D. J. Diamond, L. Neymotin, P. Kohut

Brookhaven National Laboratory
Upton, NY 11973-5000

D. D. Ebert, NRC Project Manager

Prepared for
Division of Systems Technology
Office of Nuclear Regulatory Research
U.S. Nuclear Regulatory Commission
Washington, DC 20555-0001
NRC Job Code W6382

ABSTRACT

A study was undertaken of power excursions in high burnup cores. There were three objectives in this study. One was to identify boiling water reactor (BWR) and pressurized water reactor (PWR) transients in which there is significant energy deposition in the fuel. Another was to analyze the response of BWRs to the rod drop accident (RDA) and other transients in which there is a power excursion. The last objective was to investigate the sources of uncertainty in the RDA analysis. In a boiling water reactor, the events identified as having significant energy deposition in the fuel were a rod drop accident, a recirculation flow control failure, and the overpressure events; in a pressurized water reactor, they were a rod ejection accident and boron dilution events. The RDA analysis was done with RAMONA-4B, a computer code that models the space-dependent neutron kinetics throughout the core along with the thermal hydraulics in the core, vessel, and steamline. The results showed that the calculated maximum fuel enthalpy in high burnup fuel will be affected by core design, initial conditions, and modeling assumptions. The important uncertainties in each of these categories are discussed in the report.

TABLE OF CONTENTS

Page

ABSTRACT iii
LIST OF FIGURES vi
LIST OF TABLES vii
EXECUTIVE SUMMARY ix
ACKNOWLEDGMENTS xi

1 INTRODUCTION 1
1.1 Background 1
1.2 Scope of Study 1
1.3 Organization of Report 2

2 TRANSIENTS/ACCIDENTS LEADING TO FUEL ENTHALPY INCREASES 3
2.1 Introduction 3
2.2 BWR Events 3
2.3 PWR Events 7

3 CALCULATIONAL METHODOLOGY FOR BWR ANALYSIS 11
3.1 Description of RAMONA-4B 11
3.2 BWR Reactor Model 13

4 ANALYSIS OF BWR TRANSIENTS/ACCIDENTS 21
4.1 The Rod Drop Accident (RDA) 21
4.2 Initial Conditions for RDA Analysis 21
4.3 Analysis of Rod Drop Accidents 27
4.3.1 Results for a Medium Burnup Core 27
4.3.2 Results for a Pseudo High Burnup Core 34
4.4 Sources of Uncertainty in RDA Analysis 39
4.5 Analysis of Thermal-Hydraulic Transients 42
4.5.1 MSIV Closure 42
4.5.2 Failure of a Recirculation Flow Controller 44

5 REFERENCES 53

Appendix A Generation of Neutronic Data A-1
Appendix B Control Rod Worth From A Specific Rod Pattern B-1
Appendix C Evaluation of the Moderator Temperature Reactivity Coefficient C-1

LIST OF FIGURES

Figure No.		Page
2.1	Fuel Enthalpy vs. Steady State Power	5
3.1	Schematic of RAMONA-4B Model	12
3.2	Neutronic Cell Layout for Half-Core Model	14
3.3	Radial Burnup Distribution (GWd/t) for Medium Burnup Model	15
3.4	Axial Burnup Distribution for Medium Burnup Model	16
3.5	Radial Power at Rated Conditions	17
3.6	Axial Power at Rated Conditions	18
4.1	Initial Control Rod Pattern for RDA Analysis	23
4.2	Radial Power at Cold Conditions	25
4.3	Axial Power at Cold Conditions	26
4.4	Power and Rod Position During RDA (Medium Burnup Case)	28
4.5	Reactivity Components During RDA (Medium Burnup Case)	29
4.6	Radial Power Distribution During RDA (Medium Burnup Case)	30
4.7	Void Fraction During RDA (Medium Burnup Case)	32
4.8	Maximum Fuel Bundle Enthalpy and Total Power During RDA (Medium Burnup Case)	33
4.9	Maximum Fuel Bundle Enthalpy vs. Burnup (Medium Burnup Case)	35
4.10	Power During RDA (Pseudo High Burnup Case)	36
4.11	Reactivity Components During RDA (Pseudo High Burnup Case)	37
4.12	Maximum Fuel Bundle Enthalpy vs. Burnup (Pseudo High Burnup Case)	38
4.13	Maximum Fuel Bundle Enthalpy During RDA Without Moderator Temperature Feedback	41
4.14	Pressure and Void Fraction During MSIV Closure Event	43
4.15	Power and Void Fraction During MSIV Closure Event	45
4.16	Reactivity Components During MSIV Closure Event	46
4.17	Fuel Enthalpy and Temperature During MSIV Closure Event	47
4.18	Power and Flow During Recirculation Flow Transient	48
4.19	Reactivity Components During Recirculation Flow Transient	49
4.20	Axial Power Distribution During Recirculation Flow Transient	50
4.21	Power and Enthalpy During Recirculation Flow Transient	51
A.1	Assembly and Fuel Types by Axial Zones	A-4
B.1	Core Layout During Banked Position Withdrawal Sequence	B-2
C.1	Layout of an 8 x 8 Fuel Bundle	C-2
C.2	Fuel Bundle Moderator Temperature Coefficient	C-5

LIST OF TABLES

Table No.		Page
2.1	List of Events Analyzed in the Peach Bottom Updated FSAR	6
2.2	Core Average Fuel Enthalpy for Different Transients	7
2.3	List of Events Analyzed in the Zion Updated FSAR	8
2.4	Core Average Fuel Enthalpy for Different Transients	9
4.1	Reactor Model Parameters for Medium and High Burnup RDA Cases	22
4.2	Static RAMONA-4B Calculations of Rod Worth	24
4.3	Reactor Model Parameters for Thermal-Hydraulic Transients	42
A.1	Two-Group Cross Section Representation	A-2
A.2	Statepoints for Fuel Assembly Calculations	A-5
C.1	Cases Run to Assess Moderator Temperature Coefficient and Components	C-3
C.2	MTC for an 8x8 Fuel Bundle with $V=\alpha=0\%$	C-3
C.3	MTC for an 8x8 Fuel Bundle with $V=40\%$, $\alpha=0\%$	C-4
C.4	MTC for an 8x8 Fuel Bundle with $V=70\%$, $\alpha=0\%$	C-4

EXECUTIVE SUMMARY

A study was undertaken of power excursions in high burnup cores. There were three objectives in this study. One was to identify boiling water reactor (BWR) and pressurized water reactor (PWR) transients in which there is significant energy deposition in the fuel. Another was to analyze the response of BWRs to the rod drop accident (RDA) and other transients in which there is a power excursion. The last objective was to investigate the sources of uncertainty in the RDA analysis.

A review of BWR and PWR transients and accidents was done to identify potentially significant power excursions and make recommendations as to which events should be studied in more detail as a result of NRC concerns about high burnup fuel. It is already well-established that the rod drop accident in a BWR and the rod ejection accident (REA) in a PWR are important to consider because of the significant increase in fuel enthalpy during the accident. Recent experiments with high burnup fuel suggest that it may be necessary to consider events leading to relatively low fuel rod enthalpies of approximately 30 cal/g. The review was based solely on analysis already carried out for Safety Analysis Reports. It was determined that for a BWR, a recirculation flow control failure (with increasing flow) should be studied in more detail. Next in importance are any of the overpressurization events, although it is not known a priori which overpressurization event would lead to the highest enthalpy rise. If PWR events other than the rod ejection accident are to be investigated in more detail, the highest priority should be to consider boron dilution events rather than the traditional design-basis events. These are currently considered beyond-design-basis events based on their frequencies of occurrence. However, these frequencies may increase to the level of design-basis events if the consequences of interest are much lower fuel enthalpies rather than the current acceptance criterion of 280 cal/g. It was noted in this review that, because fuel enthalpy at operating conditions is significant, it is important to make the distinction between the peak enthalpy increase and the peak total enthalpy and to consider both in the context of fuel behavior. This consideration is not as important for the RDA and REA where the initial fuel enthalpy is small.

Calculations were carried out for several BWR events: an RDA, a closure of main steam isolation valves, and a recirculation pump controller failure. These calculations were done with the RAMONA-4B code and a model for a BWR/4 with a core having bundle burnups up to 30 GWd/t. The RDA calculations were also repeated for a pseudo high burnup core with bundle burnups up to 60 GWd/t. The latter model was generated as an approximation to a high burnup core.

The RDA calculations assumed initial thermal-hydraulic conditions and control rod pattern so that the worth of a control rod dropping out of the core was approximately 950 pcm. The maximum increase in fuel bundle enthalpy in the core was found to be less than 70 cal/g for the medium burnup core and less than 100 cal/g for the high burnup core. This is low relative to existing acceptance criteria for this event. However, it is larger than what might be of interest in high burnup fuel as a result of the recent experimental tests--namely, 30 cal/g. The enthalpy rise was determined not only by the dropped rod worth and the magnitude of the feedback but also by the timing of the feedback. With large subcooling, the generation of void feedback is delayed, and the fuel enthalpy continues to rise after the initial increase in enthalpy due to the power pulse.

The calculations were used to determine the increase in fuel enthalpy as a function of burnup and the effect of certain modeling assumptions. The results of the calculations were consistent with the expectation that the peak fuel enthalpy in any axial location of any bundle would be a complicated function of the control rod worth, the distance of the bundle from the dropped control rod, and the burnup at that location. The implication of this is that high burnup in a fuel bundle does not inherently limit the enthalpy rise.

A number of uncertainties were identified in the RDA analyses. They are the result of variability in the initial conditions as well as uncertainty in parameters used in the neutronic and thermal-hydraulic models. The initial conditions that are important are the control rod pattern and core temperature and

pressure (or subcooling). The control rod pattern can be any of those found during the normal withdrawal sequence which is usually based on the General Electric-recommended banked position withdrawal sequence. Consideration can also be given to patterns with a single failure during the withdrawal sequencing and with out-of-service rods in different positions. The patterns that are relevant are any in which a control rod drive has moved halfway or more out of the core so that a dropped rod situation becomes possible.

The initial coolant temperature and pressure for the RDA should be consistent with (or more conservative than) that expected at the time during startup corresponding to the particular pattern being used. The amount of subcooling and the temperature of the coolant are important for several reasons. An increase in subcooling delays the time at which coolant voiding occurs, and the corresponding negative reactivity helps shut down the power excursion. High subcooling and low temperature lead to an addition of positive reactivity during the period that the moderator heats up. The positive moderator temperature feedback is higher in higher burnup bundles and, therefore, could impact the results. Keeping the coolant subcooled also decreases the heat transfer out of the fuel relative to the 2-phase case. This tends to impact the enthalpy increase after the initial power rise is over.

The uncertainties in modeling that are of particular importance with high burnup fuel are the result of the rim effect. The rim effect is the large increase in plutonium concentration and power along the surface of the fuel pellet. Reactor physics models that generate cross sections make assumptions about the temperature and power distributions across the pellet which may be inconsistent with the actual conditions at high burnup and, therefore, may introduce additional uncertainty. These models may also be deficient if they do not track the higher actinides which are present in high burnup fuel.

The rim effect introduces a spatial distribution of thermal properties that may be important. The neglect of this introduces uncertainty as does incorrect assumptions about the distribution of energy deposition within the pellet. Note too that the thermal properties change with burnup, and the accuracy of these properties affects the results.

The increase in fuel enthalpy during the period of the RDA after the power pulse and before steam voids have added negative reactivity can be significant. One factor that affects the enthalpy rise is the timing of void generation. The void generation models in codes used for RDA analysis are based on experiments that do not mimic the dynamic conditions of an RDA. Although this is a source of uncertainty in the analysis, it is difficult to ascertain how large this effect would be without improved data and models.

One additional, and potentially large, source of uncertainty is the power peaking factor that is used to calculate maximum fuel rod enthalpy given the maximum bundle-average fuel enthalpy at a particular axial position. The peaking factor is an approximate means of accounting for the power distribution in the bundle. It is usually taken from a single-bundle calculation and, therefore, does not account for the actual environment of the bundle, i.e., it does not account for global power tilts.

The calculations of thermal-hydraulic (non-RDA) transients carried out for this study included one transient initiated by closure of main steam isolation valves and one initiated by a recirculation flow controller failure. The results show that the fuel enthalpy increase is small and takes place over a long time interval relative to the case of an RDA. The significance of these numbers will be assessed as more data on fuel behavior become available.

In summary, this study has looked at what power excursions might be important in light water reactors and has carried out calculations of the RDA and two thermal-hydraulic transients in a BWR. The calculations have been used to determine the fuel enthalpy increase in high burnup cores and to understand the effect of burnup on the enthalpy rise. The study has also looked at the effect of the calculational methodology on the uncertainty in the results.

ACKNOWLEDGMENTS

The authors wish to thank Drs. David D. Ebert and Ralph O. Meyer of the U.S. Nuclear Regulatory Commission for their support of this project and for supplying additional technical expertise. They also wish to thank Ms. Jean M. Frejka for preparing the final report and Ms. Cheryl S. Conrad for generating the figures.

1 INTRODUCTION

1.1 Background

Reactivity-initiated accidents and certain design-basis transients lead to power excursions which are considered acceptable if they meet specified acceptance criteria. For rapid power excursions, these criteria are based on the energy deposition in the fuel pellet (which is approximately equal to the fuel enthalpy). The criteria were defined, in part, on the basis of experiments done on fuel with zero or low burnup. In recent years, experiments have been performed to examine the behavior of high burnup fuel subjected to a power pulse. Some fuel has failed at energy depositions that are low relative to the acceptance criteria. Furthermore, other recent studies of high burnup fuel show that property changes, at the surface of the pellet and in the clad, could make the fuel more vulnerable to power pulses. These activities have called into question the current acceptance criteria, and new studies to address this issue have been undertaken by the light water reactor community throughout the world.

The U.S. Nuclear Regulatory Commission (NRC) has expressed its concern regarding the above in two Information Notices that have been issued: (NRC, 1994) and (NRC, 1995). In addition, the NRC sponsored a research program to improve their understanding of the situation and to see if regulatory action is needed. This program has three different thrusts. One is to study the new experimental data being collected in France, Japan, and Russia as well as the data available from measurements made in the past, especially in the U.S. This is intended to enable the NRC to better understand how burnup affects fuel behavior during power excursions. Another thrust is to improve analytical models of fuel behavior so that they are applicable at high burnup. This would enable analytical studies of fuel behavior to be completed. The third thrust, which is the subject of this report, is to review the transient/accident analysis that has been done in the past and to perform new calculations. This would enable the NRC to understand the consequences of these transients/accidents for cores with high burnup fuel.

1.2 Scope of Study

There are three specific objectives in this study. One is to identify boiling water reactor (BWR) and pressurized water reactor (PWR) transients in which there is significant energy deposition in the fuel. Another is to analyze the response of BWRs to the rod drop accident (RDA) and other relevant transients. The last objective is to investigate the sources of uncertainty in the RDA analysis.

The first objective was carried out by reviewing calculations of events that are reported in plant safety analysis reports. Specific events in which there is energy deposition in the fuel were identified and ranked according to the increase in fuel enthalpy. Thermal-hydraulic transients that cause a power increase were considered as well as events in which there is movement of control rods or changes in boron concentration.

The second objective, the calculation of specific events, required the setting up of a BWR model for use by the RAMONA-4B code. Two models were developed: one based on plant data for a BWR/4 at the end of a typical cycle with medium burnup fuel and one based on an extrapolation of that core to high burnup conditions. These models required extensive fuel bundle calculations in order to obtain the required cross sections. The calculations of the RDA and thermal-hydraulic transients gave the increase in fuel enthalpy in bundles with different burnups. Each calculation of fuel enthalpy has an

uncertainty associated with it, and to satisfy the third objective of the study, the sources of uncertainty for the RDA are discussed in the report.

1.3 Organization of Report

In Section 2, there is a review of BWR and PWR transients/accidents which might lead to significant fuel enthalpies. Recommendations are made for further study of power excursion events. Sections 3 and 4 then focus on the analysis of BWR events of interest. Section 3 provides information on the methodology used to do the analysis for this study, and Section 4 contains the results of the analysis itself. The analysis includes calculations of both the rod drop accident (RDA) and certain thermal-hydraulic events. Section 4 also contains a discussion of sources of uncertainty in the analysis of the RDA. Appendices contain important information peripheral to the main thrust of the report. Appendix A gives details of how the neutron cross sections are obtained, Appendix B describes a calculation of control rod worth from a specific control rod pattern, and Appendix C discusses the positive moderator temperature coefficient of high burnup fuel bundles at cold conditions.

2 TRANSIENTS/ACCIDENTS LEADING TO FUEL ENTHALPY INCREASES

2.1 Introduction

A review of BWR/PWR transients/accidents has been performed to identify events in which the energy deposition may be significant. Significant for this study means that the event leads to a peak fuel enthalpy increase considerably less than has been of concern in the past. Interest in low fuel enthalpies comes about because of recent tests that show some high burnup fuel failures at lower energy depositions.

In the past, it has only been the reactivity-initiated design-basis accidents which have been considered to lead to significant energy depositions. These events, the rod drop accident (RDA) in a BWR and the rod ejection accident in a PWR, have been the only ones analyzed in the past with the intention of comparing the calculated fuel enthalpy in the core with the limit of 280 cal/g for unacceptable fuel damage. These events are still of interest, but events with much lower fuel enthalpies are of interest now as well.

In order to assess the maximum fuel enthalpy during a design-basis transient/accident without doing an independent calculation of the event, the following scheme was used. For many events, analysis has been done and selected results presented in Final Safety Analysis Reports (FSARs). One of the parameters that is almost always shown in graphical form is the total core power vs. time. If this quantity is integrated over time, then the total energy deposition during the event is known. Energy deposition can be converted into the core fuel enthalpy increase (cal/g), assuming no heat loss into the coolant, by dividing by the total amount of UO_2 in the core.

This approach was applied to both a BWR and a PWR, but it has several drawbacks. The most important is that the maximum fuel enthalpy in the core must take into account the distribution throughout the core, which is not available in the FSAR. Hence, an estimated peaking factor must be used. Another drawback is that this approach assumes that the process is adiabatic and that all energy deposited in the fuel goes to increase the fuel enthalpy and that there is no heat transfer to the coolant. This leads to an overestimate of the fuel enthalpy but is not considered a major drawback. Another problem is that the events given in the FSAR are generally the most limiting in terms of critical heat flux and are not necessarily the most limiting in terms of energy deposition in the fuel. However, in events where there is a power increase, it is likely that there is a direct correlation between these two types of limiting conditions, and this should not be decisive in missing important events. Another limitation is that considering only the events in the FSAR excludes certain beyond-design-basis events that may be of some interest.

2.2 BWR Events

The review of FSAR events was done using analysis for Peach Bottom Atomic Power Station Units 2 and 3. This plant was chosen because (1) it is a BWR/4 design and the analysis carried out for this study (cf Section 3) uses a model for a BWR/4 and (2) because the FSAR had been formally "Updated" with some sections being as recent as 1991.

Transients/Accidents

The events considered are listed in Table 2.1. The list is organized as in the FSAR with abnormal operational transients categorized according to the effect in the core (Categories A-F) followed by design-basis accidents (Category G). The thermal-hydraulic events that might lead to a power increase are the result of an overpressurization (A), a water temperature decrease (B), or a flow increase (F). Events in Categories D and E are not expected to be of interest to this study.

After reviewing the power increase for each event, the four listed in Table 2.2 were identified as leading to the largest increases in core average enthalpy (after the RDA which leads to a peak fuel enthalpy of approximately 125 cal/g for a dropped rod worth 0.01 in reactivity). Note that none of the events are from Category C, Events Resulting in a Positive Reactivity Insertion. The events are listed in order of decreasing change in enthalpy. Each event leads to the minimum margin to critical power ratio at a specific initial power, and hence, the results given in the FSAR are for that particular initial condition. The initial core average fuel enthalpy as a function of power level can be estimated by assuming that the average fuel temperature increases linearly from the average coolant temperature of 285°C at zero power to a value of 650°C at full power. The resulting initial fuel enthalpy is given in Figure 2.1 and can be used approximately for PWRs as well. Since events that start from a significant power level have a significant initial fuel enthalpy, it is important to make a distinction between the incremental fuel enthalpy and the total fuel enthalpy when trying to predict fuel behavior. Table 2.2 also shows the incremental and total enthalpy for the four events listed.

Since the numbers in Table 2.2 are obtained on a core-average basis, a peaking factor can be applied to determine the peak fuel enthalpy during the event. This peaking factor may be 2-3, and, therefore, the enthalpy increase may be as large as 30 cal/g and the total enthalpy may be as large as 130 cal/g for the first event listed. These numbers assume an adiabatic condition and would be smaller if heat transfer to the coolant were taken into account. However, since these transients are over in less than four seconds, the adiabatic assumption is still appropriate. The overpressurization events listed in the table are similar to others with different conditions, such as different initial power or different number of main steam isolation valves (MSIVs) closing. For other plants, it is just as likely that a different overpressurization event would be listed in this table.

In addition to those transients/accidents analyzed in the FSAR, consideration can be given to other types of events, so-called beyond-design-basis events. One such event is the result of being in the operating domain where the core is unstable and oscillations occur. If these oscillations do not immediately cause reactor trip or there is no operator action taken, then fuel enthalpy may increase. The worst situation envisioned would be for asymmetric oscillations leading to high power in one region in the core while the core average power is still at reasonable levels.

Other beyond-design-basis reactivity accidents have been studied in the past (Diamond, 1990). The priority for studying these events is less than for studying the events considered above. These events include:

1. overpressurization events in which there was failure of either some relief valves, or recirculation pump trip, or reactor trip,

2. anticipated transients without scram (ATWS events) with the injection of cold emergency core cooling system (ECCS) water after the core is shutdown from actuation of the standby liquid control system, and

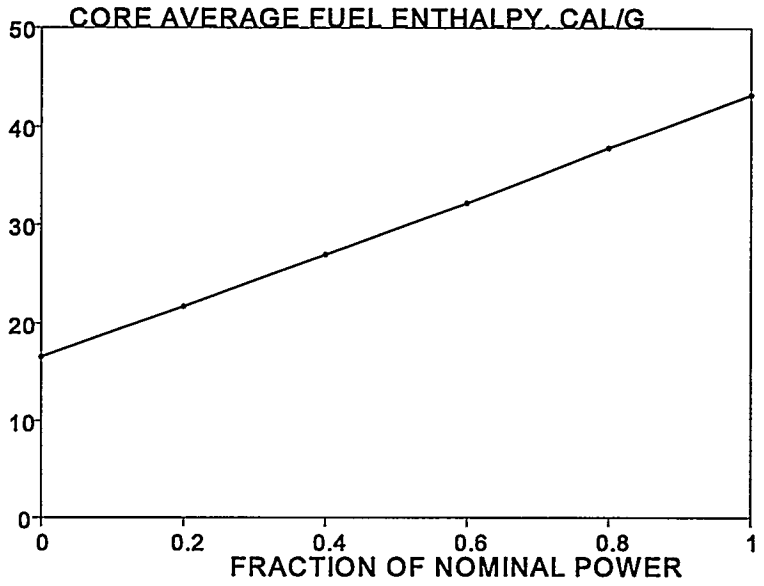

Figure 2.1 Fuel Enthalpy vs. Steady-State Power

Table 2.1 List of events analyzed in the Peach Bottom Updated FSAR

A.	**Events Resulting in a Nuclear System Pressure Increase**
1.	Electrical load rejection (Turbine control valve fast closure)
2.	Turbine trip (Turbine stop valve closure)
3.	Main steam line isolation valve closure
B.	**Events Resulting in a Reactor Vessel Water Temperature Decrease**
4.	Inadvertent pump start
5.	Feedwater controller failure - maximum demand
6.	Loss of feedwater heating
7.	Shutdown cooling (RHRS) malfunction - decreasing temperature
C.	**Events Resulting in a Positive Reactivity Insertion**
8.	Continuous rod withdrawal during power range operation
9.	Continuous rod withdrawal during reactor startup
10.	Control rod removal error during refueling
11.	Fuel assembly insertion error during refueling
D.	**Events Resulting in a Reactor Vessel Coolant Inventory Decrease**
12.	Pressure regulator failure
13.	Inadvertent opening of a relief valve or safety valve
14.	Loss of feedwater flow
15.	Loss of auxiliary power
E.	**Events Resulting in a Core Coolant Flow Decrease**
16.	Recirculation flow control failure - decreasing flow
17.	Trip of one recirculation pump
18.	Trip of two recirculation motor-generator set drive motors
19.	Recirculation pump seizure
F.	**Events Resulting in a Core Coolant Flow Increase**
20.	Recirculation flow controller failure - increasing flow
21.	Startup of idle recirculation pump
G.	**Analysis of Design-Basis Accidents**
22.	Control rod drop accident
23.	Loss-of-coolant accident
24.	Refueling accident
25.	Main steam line break accident

Table 2.2 Core average fuel enthalpy for different transients

Transient	Initial Power, % Full Power	Enthalpy Increase, cal/g	Total Enthalpy, cal/g
Recirculation flow control failure - increasing flow	67	9.6	43.8
Turbine trip without bypass	30	5.1	29.5
Closure of one MSIV	100	1.6	44.8
Turbine trip with bypass	100	1.3	44.5

3. refueling accidents in which loading takes place in a region of the core with control rods removed.

2.3 PWR Events

The review of FSAR events was done using analysis for the Zion Station. This plant was chosen because the FSAR had been formally "Updated" with some sections being as recent as 1992.

The events considered are listed in Table 2.3. The list is organized as in the FSAR with categories of events according to the general effect in the core. The thermal-hydraulic transients that might lead to an increase in power are primarily in Category A, Increase in Heat Removal by the Secondary System. However, an examination of the events in this category shows that the increase in fuel enthalpy is insignificant. Events in Categories B, C, E, and F are not expected to be of interest to this study.

The events in Category D, Reactivity and Power Distribution Anomalies, are the ones that are significant for a PWR, and the rod ejection accident falls into this category and leads to a peak fuel enthalpy of less than 200 cal/g. Other events which might be considered are listed in Table 2.4.

For the rod withdrawal from a subcritical condition, the increase in the core average fuel enthalpy is 16 cal/g over an 8-second time interval. However, since this transient is slow, the effect of heat transfer to the coolant is expected to become important, and the table instead gives the enthalpy increase out to four seconds. The corresponding total enthalpy would be 25 cal/g as initially the core is at hot zero power conditions. For this event, the appropriate peaking factor to apply is dependent on the initial control rod pattern and the control rod withdrawn. Typically, the peaking factor can increase by 2-3, and if this is applied to the increase in enthalpy, the total enthalpy can be as high as 50 cal/g.

Table 2.3 List of events analyzed in the Zion Updated FSAR

A.	**Increase in Heat Removal by the Secondary System**
1.	Excessive heat removal due to feedwater system malfunctions
2.	Feedwater system malfunctions that result in an increase in feedwater flow
3.	Excessive load increase incident
4.	Inadvertent opening of a steam generator relief or safety valve
5.	Depressurization of the main steam system
B.	**Decrease in Heat Removal by the Secondary System**
6.	Steam pressure regulator malfunction or failure that results in decreasing steam flow
7.	Loss of external electrical load
8.	Turbine trip (stop valve closure)
9.	Inadvertent closure of main steam isolation valve
10.	Loss of condenser vacuum
11.	Loss of all AC power to the station auxiliaries
12.	Loss of normal feedwater
13.	Feedwater piping break
C.	**Decrease in Reactor Coolant System Flow Rate**
14.	Single and multiple reactor coolant pump trips
15.	Reactor coolant pump locked rotor
16.	Reactor coolant pump shaft break
D.	**Reactivity and Power Distribution Anomalies**
17.	Uncontrolled rod cluster control assembly withdrawal from a subcritical condition
18.	Uncontrolled rod cluster control assembly withdrawal at power
19.	Rod cluster control assembly misalignment
20.	Startup of an inactive reactor coolant loop
21.	Chemical and volume control system malfunction
22.	Inadvertent loading and operation of a fuel assembly in an improper position
23.	Rod cluster control assembly ejection
E.	**Increase in Reactor Coolant Inventory**
24.	Inadvertent operation of emergency core cooling system during power operation
25.	Chemical and volume control system malfunction (or operator error) that increases inventory
F.	**Decrease in Reactor Coolant Inventory**
26.	Inadvertent opening of a pressurizer safety or relief valve
27.	Break in instrument lines or other lines from reactor coolant pressure boundary that penetrate containment
28.	Steam generator tube rupture
29.	Loss of coolant accident

Table 2.4 Core average fuel enthalpy for different transients

Transient	Initial Power, % Full Power	Enthalpy Increase, cal/g	Total Enthalpy, cal/g
Uncontrolled rod withdrawal from subcritical condition	0	8.0[a]	25
Uncontrolled rod withdrawal at power - trip on high neutron flux	100	2.2	45
Startup of an inactive coolant loop	80	2.2	45[b]

[a] For first four seconds
[b] Based on starting from 100% power

The remaining events listed in Table 2.4 have only a small increase in fuel enthalpy but start from a higher initial value. During the startup of an inactive coolant loop, the power level increases slowly from 80 percent to 100 percent and then undergoes an excursion which results in the enthalpy increase given. The total enthalpy is based on starting from 100 percent power.

There are also beyond-design-basis events for the PWR that can be considered. Of particular interest are boron dilution events that have been studied in recent years. In the past, frequencies were calculated for events with a large boron dilution to achieve a fuel enthalpy of more than 280 cal/g. With a smaller fuel enthalpy criterion, a smaller dilution is required and some of these events may have frequencies of occurrence that are in the same range as design-basis accidents. One example of such an event (Diamond, 1992) is initiated during restart if there is a loss-of-offsite power when the reactor is being deborated. Another example (Nourbakhsh, 1994) occurs during a small break loss-of-coolant accident if there is reflux condensation. Since these events could lead to significant increases in fuel enthalpy, they may be more important than the events listed in Table 2.4.

3 CALCULATIONAL METHODOLOGY FOR BWR ANALYSIS

3.1 Description of RAMONA-4B

RAMONA-4B (Wulff, 1984) is a systems transient code for boiling water reactors. The code uses a 3-dimensional neutron kinetics model coupled with a multichannel, 2-phase flow model of the thermal hydraulics in the reactor vessel. The 3-dimensional neutron kinetics makes the code well-suited for predicting transients and accidents where the spatial core power variations are expected to be significant. The code is designed to analyze a wide spectrum of BWR core and system transients. The four major classes of transients/accidents are the following:

(1) reactivity transients driven by control rod actions and boron injection,
(2) system pressure transients: load rejection, turbine trip, main steam isolation valve (MSIV) closure, and failure of pressure regulator,
(3) coolant inventory transients, and
(4) coolant temperature transients.

A schematic of the BWR, which can be modeled with RAMONA-4B, is shown in Figure 3.1. It consists of a feedwater sparger, upper and lower downcomers, a combined recirculation loop with recirculation and jet pumps, a lower plenum, a core, a riser, including an upper plenum and steam separator stand-pipes, a steam dome, and a steamline with safety/relief valves, main steam isolation valve, turbine bypass valve, and turbine stop valve. The code also has models for a plant protection system, a safety injection system, and certain control systems.

The reactor core is modeled with multiple parallel coolant channels and a bypass channel. Each coolant (i.e., thermal-hydraulic) channel is interfaced with one or more fuel bundles. The reactor power, including decay heat, is calculated in 3-dimensional geometry. The fission power calculation takes into account control rod movement (including accidental rod drop and reactor trip) and the feedback throughout the core due to changes in the fuel and coolant temperatures and steam void fraction. Energy deposited directly into the coolant and bypass channels is taken into account. Thermal conduction through the fuel pellet, gas gap, and fuel cladding is modeled to obtain the heat transfer from the fuel to the coolant.

The neutron kinetics model of RAMONA-4B is based on 2-group diffusion theory with six delayed neutron precursor groups. Simplifications are made in treating the thermal neutron flux to reduce the formulation to a 1½-group, coarse mesh diffusion model in a 3-dimensional rectangular coordinate system. Each mesh box in the x-y plane contains a single fuel bundle. Neutronic boundary conditions are specified at the axial and radial core periphery.

The partial differential equations are first transformed into ordinary differential equations in time. The initial, or steady-state conditions, are obtained by setting the time derivatives to zero and iterating to obtain the eigenvalue, $1/k_{eff}$, of the system of equations. For transient calculations, an implicit time differencing scheme with Gauss-Seidel iteration is used to integrate the prompt neutron kinetics equations; the delayed neutron equations are integrated by using an explicit method.

The thermal-hydraulic calculation in RAMONA-4B is based on a 4-equation, nonequilibrium, drift-flux model. The four balance equations are: conservation of (1) vapor mass, (2) mixture mass, (3) mixture momentum, and (4) mixture energy. Two-phase mixture is allowed in the downcomer, lower plenum,

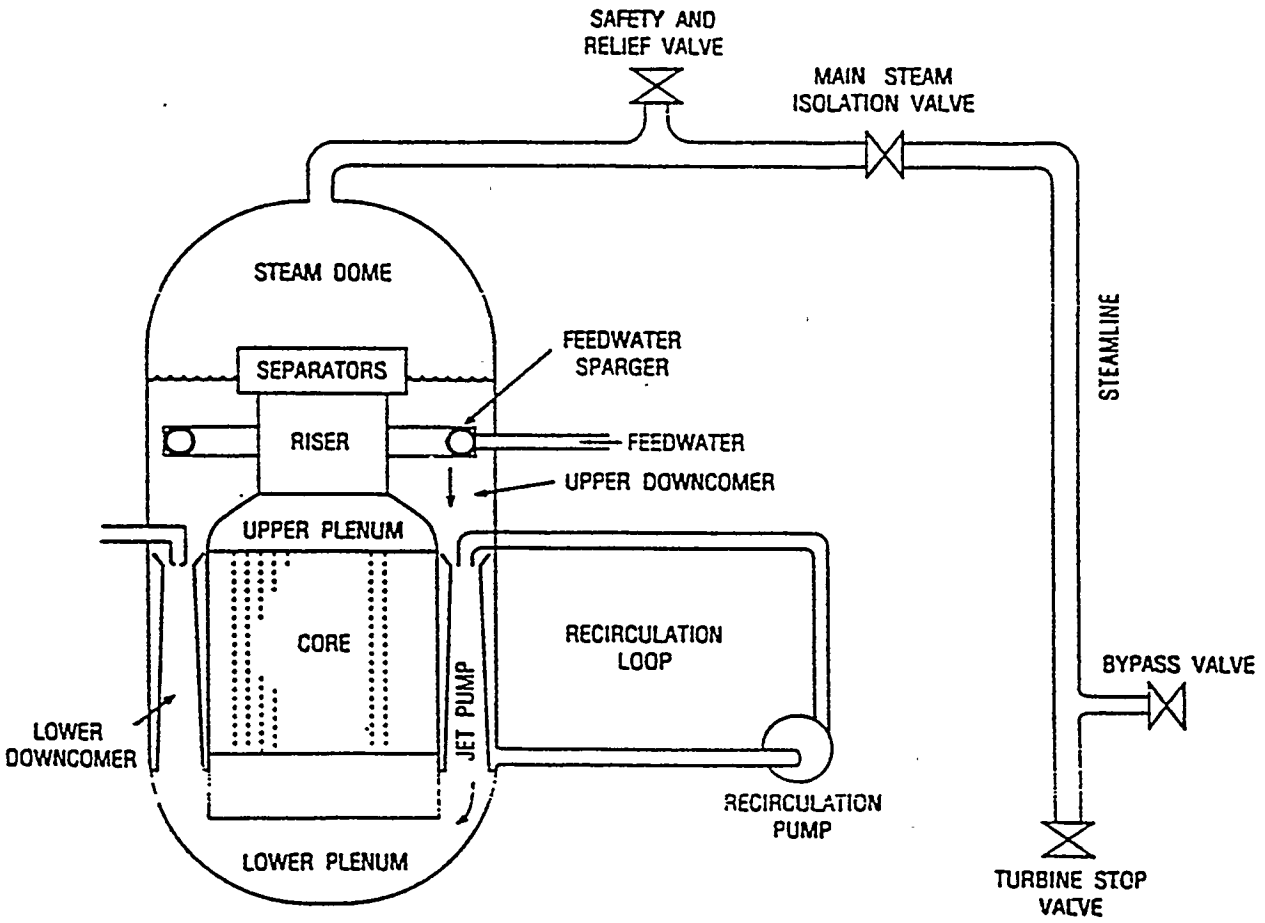

Figure 3.1 Schematic of RAMONA-4B Model

core, and riser. The steam dome (above the 2-phase mixture level) is occupied by saturated vapor, whereas the recirculation loop is assumed to contain only single-phase liquid.

Elevations of the mixture and collapsed water levels in the downcomer/steam dome region are calculated. Prediction of the collapsed water level is important since the feedwater and the safety injection systems, high pressure coolant injection, and reactor core isolation cooling are controlled based on the water level. A standby liquid control system for injecting highly concentrated borated water into the reactor vessel also is modeled, and the code integrates the boron transport equation to calculate the boron concentration as a function of space and time.

Steamline dynamics between the reactor vessel and turbine is accounted for by solving the vapor mass and momentum conservation equations. Adiabatic expansion and/or compression of steam is assumed in the steamline model. Models for the safety/relief valves, main steam isolation valves, and turbine bypass and stop valves are included. The code has a model for the pressure regulator.

A plant protection system designed to control the reactor during abnormal transients and accidents is modeled. This system includes the reactor scram and turbine and recirculation pump trips based on transient time (user input) or setpoints for the thermal-hydraulic and neutronic system parameters.

3.2 BWR Reactor Model

A BWR/4 reactor core was modeled using half-core mirror symmetry. Figure 3.2 shows the core layout. The model included 382 neutronic channels where each channel represented a single fuel bundle. These are the boxes shown on the figure. The core model included 100 control rods which are located at the center of the boxes with four fuel bundles outlined in solid lines on the figure. The use of half-core symmetry allowed for the dropping of any control rod along the axis of symmetry. (Any other control rod movement would imply the movement of two rods due to the symmetry.) The number of calculational nodes in the vertical direction was 24.

The thermal hydraulics of the core region was modeled using 160 channels associated with fuel bundles and one bypass channel representing the area between the bundles. These channels are marked on Figure 3.2. The majority of the thermal-hydraulic channels were "shared" by several neutronic channels. The thermal energy released in those several neutronic channels was collectively deposited into the liquid flowing in that particular thermal-hydraulic channel. Each of the neutronic channels in three rows of bundles adjacent to the core's axis of symmetry had a dedicated thermal-hydraulic channel in order to most accurately represent the thermal-hydraulic reactivity feedback effects (void fraction and moderator and fuel temperature) following a control rod drop.

Two cores were modeled. One, described as a medium burnup core, had fuel bundles with burnups up to a maximum of approximately 30 GWd/t. The cross sections for this core had been generated using the CASMO code (Ahlin, 1978) for a previous study (Valtonen, 1992). The average radial and axial distributions of burnup in the core are shown in Figures 3.3 and 3.4, respectively. Figure 3.4 also shows the axial distribution in one particular bundle along the axis of symmetry. The resulting radial and axial power distributions for full power operation are shown in Figures 3.5 and 3.6, respectively.

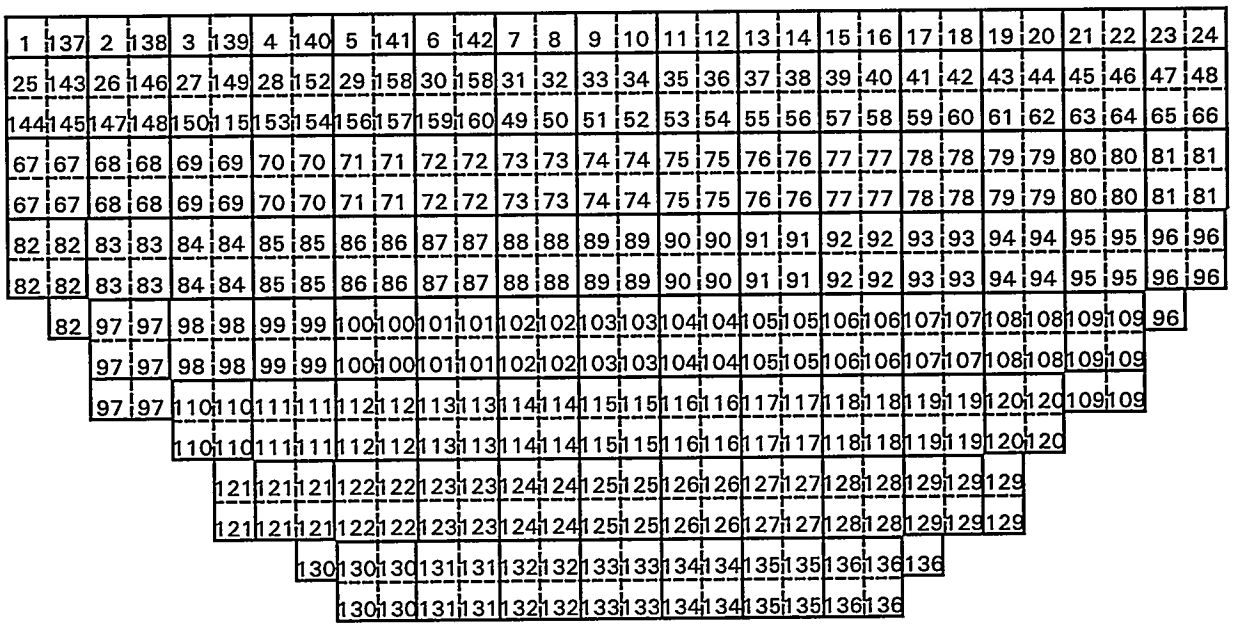

Numbers refer to thermal-hydraulic channel.

Figure 3.2 Neutronic cell layout for half core model

26.5	22.5	11.1	27.3	28.5	24.2	11.2	26.2	28.7	24.4	11.3	26.6	23.6	7.5	25.5
22.3	11.5	25.4	10.6	18.2	11.5	25.3	11.4	18.8	11.7	19.0	10.8	16.0	7.7	26.2
11.2	25.4	11.3	23.5	10.8	19.4	11.8	22.6	11.4	25.1	11.6	18.3	9.5	7.6	26.6
27.8	11.1	24.1	26.2	29.1	11.5	19.3	25.7	29.0	11.3	18.7	24.9	23.3	7.2	26.0
28.3	18.7	11.3	29.3	27.6	19.1	11.5	28.5	29.2	18.9	11.0	28.6	23.4	6.8	25.9
24.4	11.7	19.6	11.6	19.1	11.8	25.2	11.3	19.0	11.5	23.4	10.0	15.6	6.5	24.4
11.3	25.6	11.9	19.3	11.5	25.2	11.6	22.1	11.1	18.8	10.7	16.9	7.9	21.3	23.2
26.2	11.4	22.8	25.9	28.8	11.3	21.8	28.1	28.2	10.3	19.7	8.5	25.6	24.9	
28.3	18.9	11.4	29.2	29.3	19.0	11.1	28.2	28.0	16.6	8.5	6.9	24.4		
24.2	11.7	25.3	11.3	18.8	11.5	18.8	10.4	16.6	14.1	23.0	25.3	21.7		
11.2	19.3	11.6	18.9	11.0	23.5	10.7	19.4	8.6	22.8	26.5				
26.6	10.8	18.2	24.9	29.4	9.9	16.9	8.5	6.9	25.6					
23.8	16.0	9.5	23.2	23.4	15.5	7.8	25.9	24.3	21.9					
7.4	7.7	7.6	7.1	6.8	6.5	21.4	24.9							
25.7	26.3	26.6	25.6	25.4	24.6	23.1								

Figure 3.3 Radial Burnup Distribution (GWd/t) for Medium Burnup Model

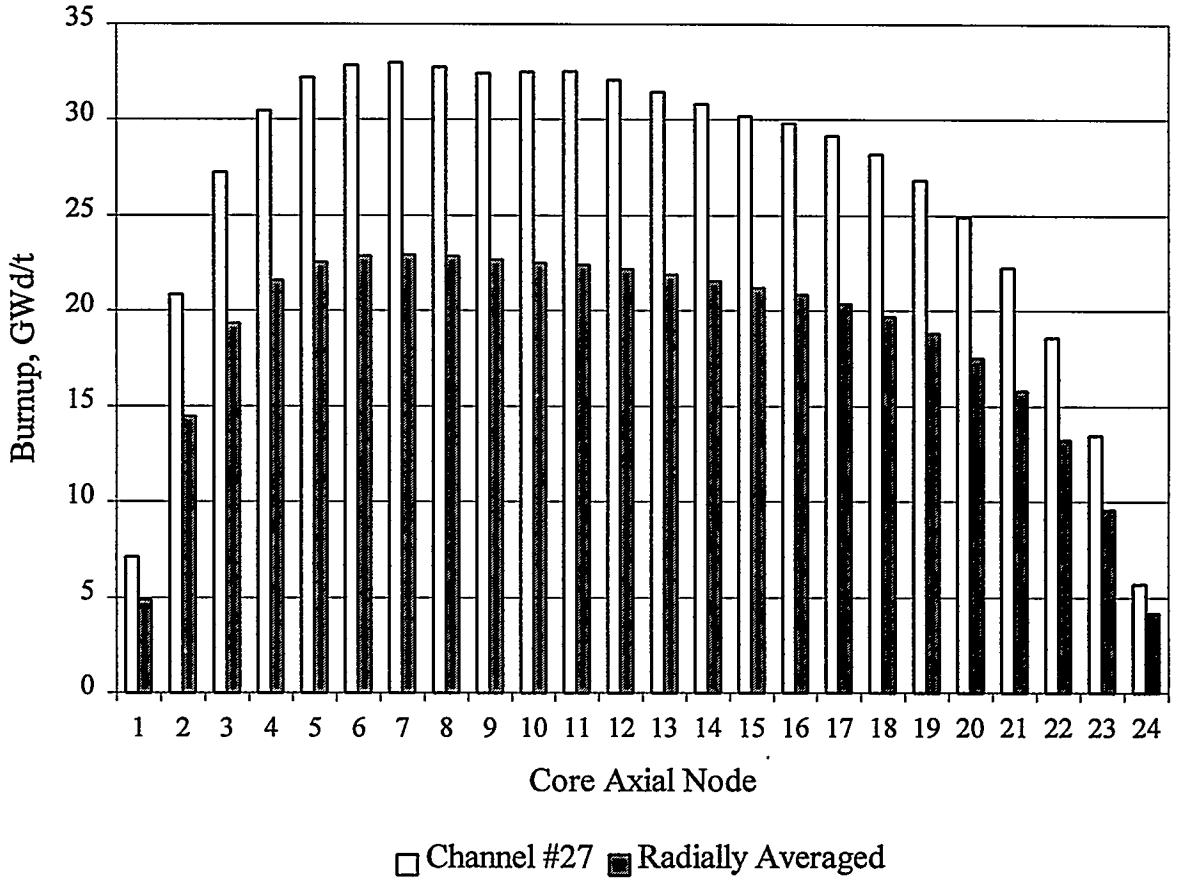

Figure 3.4 Axial Burnup Distribution for Medium Burnup Model

98	107	126	102	100	108	127	103	99	104	121	93	87	75	40
107	126	109	125	116	127	111	124	114	123	113	115	97	77	40
126	109	125	109	129	119	128	110	125	108	124	105	106	78	40
103	127	105	102	103	130	114	103	100	124	108	97	87	82	36
101	116	133	103	103	115	130	101	98	110	123	91	84	79	35
104	131	119	130	115	132	107	126	112	126	100	116	90	81	36
134	108	132	115	131	107	127	104	126	111	119	102	94	58	32
106	129	107	104	101	126	104	97	96	120	99	102	59	40	
100	114	130	101	99	112	126	97	90	98	101	82	42		
102	128	106	126	111	127	112	120	98	87	63	42	31		
131	116	131	111	125	102	120	100	102	63	42				
99	123	109	100	94	118	104	103	82	43					
94	103	116	93	89	93	96	61	43	32					
107	110	110	105	99	86	60	41							
47	46	46	45	43	38	34								

Figure 3.5 Radial Power (% of Core Average) at Rated Conditions

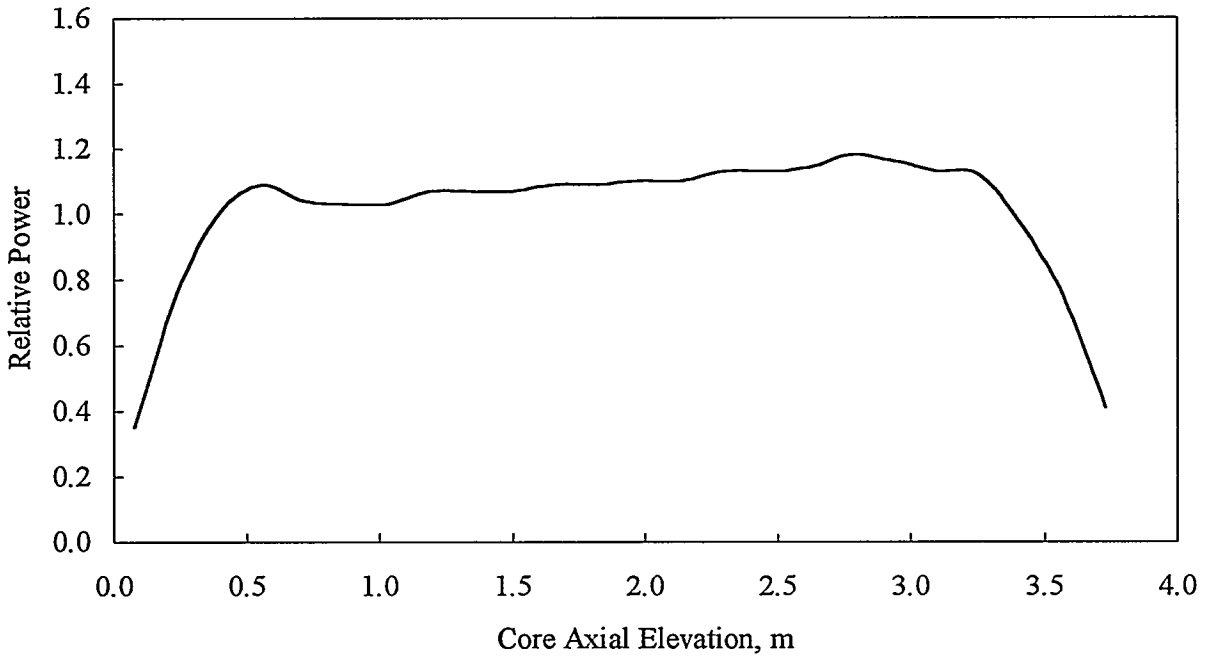

Figure 3.6 Axial Power at Rated Conditions

The other core was meant to represent the situation with bundle average burnups up to 60 GWd/t (and hence, fuel rod burnups of up to approximately 65 GWd/t). Since no data were available to the authors for actual or planned cores with this burnup, a method was used which allowed for the medium burnup data to be extrapolated to produce the high burnup core. The approach is explained in Appendix A. This new core model is only an approximation to an actual core. However, it provides sufficient information to test certain hypotheses and add to our understanding of high burnup cores.

Other key parameters which describe the BWR/4 model, including initial conditions and other modeling assumptions, are given in Sections 4.2 and 4.5 for the rod drop accident and the thermal-hydraulic transients, respectively.

4 ANALYSIS OF BWR TRANSIENTS/ACCIDENTS

4.1 The Rod Drop Accident (RDA)

For an RDA to occur, several conditions must be present. For the control rod of interest, the control rod drive must be withdrawn from the core either completely, or as will be shown below, at least from the top half of the core. The assumptions are made that the coupling between the drive mechanism and the control blade has separated and that the blade sticks in its original position. This blade then has the opportunity at a later time to unstick and fall to the position of the drive mechanism. It is also assumed that the operator does not notice a lack of neutron monitoring response as the drive is withdrawn or does not verify rod coupling if the rod is fully withdrawn. The expectation is that this is a low probability event, but no recent estimates of the frequency of occurrence exist.

The open literature has several examples of RDA calculations, e.g., (Cheng, 1981), (Belblidia, 1993), and (Grandi, 1994). Although this event has been calculated for licensing purposes and for special studies for many years, it is only recently that the methodologies utilized have changed considerably. This is due to the increase in availability of codes with 3-dimensional neutron kinetics coupled to thermal-hydraulics models.

4.2 Initial Conditions for RDA Analysis

The calculation of rod drop accidents for this study was done for both the medium and high burnup core models. Table 4.1 contains some of the neutronic and thermal-hydraulic parameters used to describe initial conditions, plant response, and modeling in RAMONA-4B for these calculations.

The initial control rod pattern with 50 percent control density, shown in Figure 4.1, was chosen for several reasons. The most important was that in a study of limited scope, it would be too difficult to search through all of the possible patterns to obtain a pattern with the highest worth dropped control rod or the worst fuel enthalpy increase. BWR reactors use systems that lead to patterns such as those in the banked position withdrawal sequence (Paone, 1977). Not only would one have to go through all the patterns possible using this system, but also patterns possible if a single failure criterion was applied and if out-of-service rods were present. Since a checkerboard pattern had been used by other analysts to study the RDA, it was hoped that using this condition would enable comparisons to be made with those other results. It resulted in control rod worths up to about 950 pcm which corresponded to rod worths obtained by other analysts using the banked position withdrawal sequence and, therefore, it was felt justified. Calculations were done with another pattern which resulted in a control rod worth that would only lead to a subprompt-critical excursion. This is explained in Appendix B.

The initial thermal-hydraulic conditions in the reactor corresponded to cold startup. The power was 10^{-6} of full power, and the core coolant temperature was 30°C. This was equivalent to 70°C subcooling at atmospheric pressure which was assumed to be the system pressure. This delays the onset of steam generation caused by the RDA and, therefore, the addition of negative void reactivity feedback which tends to mitigate the accident. The single-phase coolant decreases the heat transfer to the coolant relative to the case with 2-phase flow. This has the effect of keeping the fuel temperature (and fuel enthalpy) higher; and, as with the void reactivity, this is in the direction so as

Table 4.1 Reactor model parameters for medium and high burnup RDA cases

Parameter/Condition	Value/Description	Comment
Fuel bundle maximum burnup	30/60 GWd/t	For medium/high burnup calculations
Reactor power	3.29 kW ("zero" power)	10^{-6} of rated power
Control rod insertion pattern	Checkerboard; 50% control rod density	See Figure 4.1
Fraction of energy deposited directly into coolant	0.04	Total for the in-channel and bypass liquid
Delayed neutron fraction	0.006/0.005	For medium/high burnup calculations
Xenon inventory	Fully depleted	
Reactor trip setpoint	15% of rated power with 0.2 s delay	
Scram insertion speed	1.2 m/s (3.9 ft/s)	
Control rod drop speed	0.94 m/s (3.1 ft/s)	
System pressure	0.1 MPa	Non-condensible atmosphere
Liquid temperature	30°C	70°C subcooled
Core flow rate	3260 kg/s	25% of rated flow

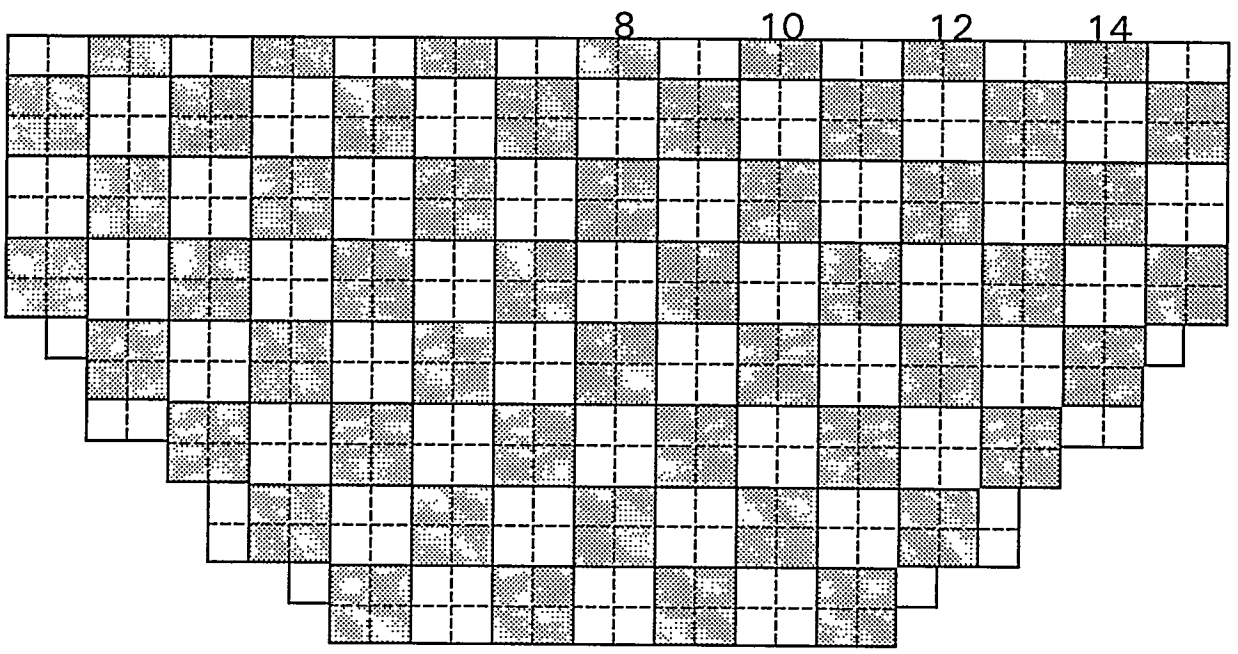

Unshaded core cells: control blade withdrawn
Shaded core cells: control blade inserted

Figure 4.1 Initial Control Rod Pattern for RDA Analysis

to make the results more severe, i.e., more limiting. The higher fuel temperature also increases the fuel temperature reactivity feedback which limits the severity of the accident, but this is expected to be a smaller effect.

The high subcooling at low initial temperature also means that coolant/moderator temperature reactivity feedback can be important. For a BWR at cold conditions, the feedback is positive and, therefore, can exacerbate the power excursion. The magnitude of the effect during an RDA is discussed in Section 4.4.

In most BWRs, the reactor becomes critical when only approximately one-fourth of the control rods are withdrawn. Hence, cold conditions would correspond to higher control rod densities than the 50 percent used in this study. At 50 percent control density, higher temperatures and pressures are expected as the power would have increased from its initial level at the cold condition. Best-estimate calculations would have to take into account the change in thermal-hydraulic conditions with changing control rod patterns. The thermal-hydraulic conditions control the positive moderator feedback, the heat transfer to the coolant, and the onset of negative void feedback. Since no information was available to the authors as to the subcooling that might be expected at different control rod patterns, the parameters used were chosen in order to make the calculations more conservative and to enable the effect of thermal-hydraulic conditions to be studied.

The initial conditions for the medium burnup core results in the radial and axial core power distributions shown in Figures 4.2 and 4.3, respectively. The power has a very high axial peaking factor which is typical of shutdown conditions in a BWR. This axial peaking tends to increase the rate of reactivity insertion when the rod drops out of the core. As will be seen in Section 4.3.1, this means that the power increases rapidly while the control rod is still in the top half of the core.

Selection of the control rod with maximum worth in the checkerboard pattern was based on results of four static RAMONA-4B calculations. In each of the calculations, one control rod (i.e., CR #8 (center), CR #10, CR #12, and CR #14; see Figure 4.1) was removed, and the corresponding eigenvalue was calculated. The results of these calculations are given in Table 4.2. The highest worth rod was CR #14 which was used to do the RDA analysis.

Table 4.2 Static RAMONA-4B calculations of rod worth

Control Rod Withdrawn	Rod Worth (pcm)
CR #8	280
CR #10	490
CR #12	680
CR #14	970

75	122	161	89	87	133	172	94	85	125	160	80	65	80	29
122	105	93	164	153	114	101	167	149	108	101	145	117	64	17
161	93	107	139	176	114	118	141	169	98	113	128	125	63	17
89	164	139	90	96	184	162	93	90	164	143	79	62	75	27
87	153	176	96	98	165	184	93	88	145	157	73	57	70	25
133	114	114	184	165	122	103	166	147	107	86	124	94	49	14
172	101	118	162	184	103	110	136	161	95	92	109	93	30	9
94	167	141	93	93	166	136	81	80	136	111	73	33	19	
85	149	169	90	88	147	161	80	71	112	107	49	16		
125	108	98	164	145	107	95	136	112	67	38	25	12		
160	101	113	143	157	86	92	111	107	38	15				
80	145	128	79	73	124	109	73	49	25					
65	117	125	62	57	94	93	33	16	12					
80	64	63	75	70	49	30	19							
29	17	17	27	25	14	9								

Figure 4.2 Radial Power (% of Core Average) at Cold Conditions

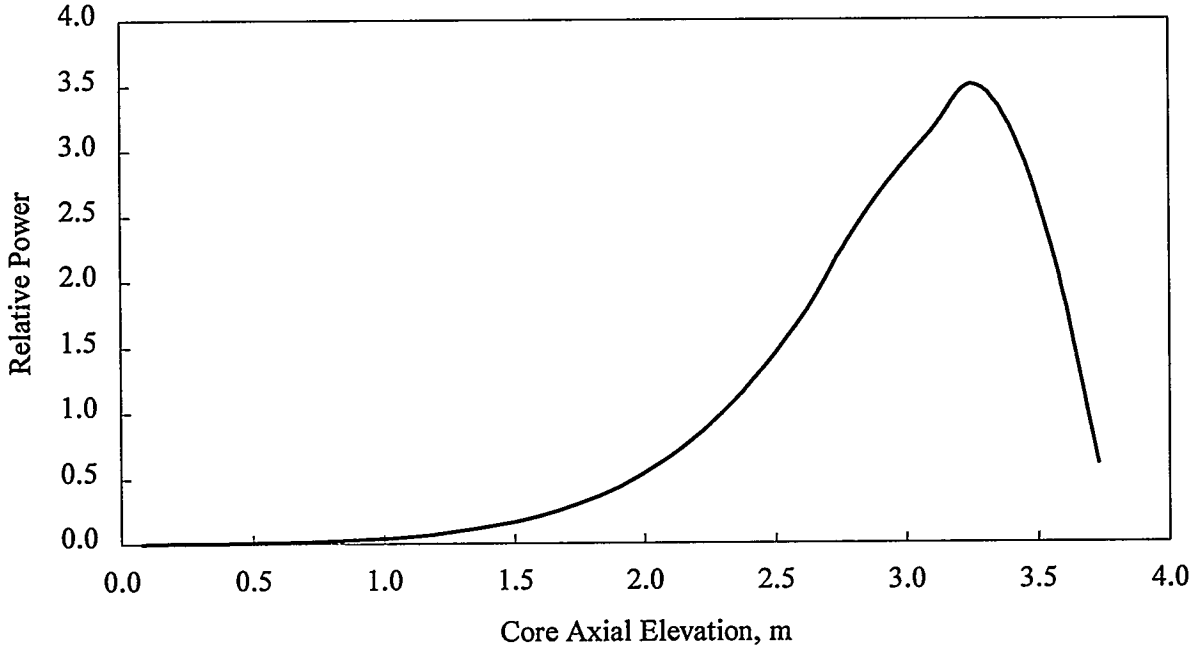

Figure 4.3 Axial Power at Cold Conditions

4.3 Analysis of Rod Drop Accidents

4.3.1 Results for a Medium Burnup Core

The accident was initiated at time zero with CR #14 dropping at a speed of 0.94 m/s (3.1 ft/s). The prompt power excursion started at about one second as can be seen in Figure 4.4, which shows the power during the transient on a logarithmic scale relative to nominal, or rated, power. The power increases more than six decades which is typical for this type of RDA.

The figure also shows the position of the control rod which is initially completely inserted. As can be seen, when the tip of the control rod traveled only three to four feet through the core, sufficient reactivity had been inserted to cause the power excursion which, in turn, was terminated by fuel temperature feedback (primarily due to the Doppler effect). This means that when realistic control patterns are considered in setting up conditions for the RDA, it is only necessary that the control rod drive mechanism be withdrawn halfway out of the core in order to set the stage for the assumption that the corresponding blade has been decoupled and has stuck so that it can later drop to the position of the drive mechanism.

The reactor power reached a peak value of approximately 2.4 of nominal power at about 1.3 seconds. At that time, the negative Doppler reactivity feedback is large enough so that the power excursion is terminated. The history of the different reactivity feedback components is shown in Figure 4.5, which also shows the power excursion on a linear scale. This figure shows that the accident can be separated into four major phases. In the first phase, reactivity is being inserted due to withdrawal of the dropped control rod. The second phase starts when the power surge is reversed due to fuel temperature (Doppler) reactivity. The third phase covers the period from the initiation of boiling in the core and its associated negative reactivity. The fourth phase occurs when the void feedback and scram become effective enough to completely shut down the core.

The plot of reactivity effects shows that the control rod worth germane to this event is approximately 750 pcm. This is 80 percent of the total static worth of the rod and primarily is the result of the fact that the rod does not withdraw all the way before the event is terminated. The figure also shows the positive reactivity feedback due to moderator heatup (discussed in more detail in Section 4.4).

Since the spatial power distribution history is important in control rod drop accidents, it is of interest to consider the 3-dimensional power distribution predicted by RAMONA-4B. Figure 4.6 shows the radial power distribution, normalized to an average power of 100, at 1.2 seconds into the event. The bulk of the energy is generated in the core region adjacent to the dropped control rod. Approximately 55 percent of total energy is generated in about 10 percent of the fuel bundles. The figure also shows that for this particular case although the peak core power is reaching toward 2.45 of nominal power, the power in an individual bundle can be a factor of 11 higher, i.e., more than 27 times the nominal average power.

The axial power distribution also changes during the transient, but because it is peaked at the top of the core initially (Figure 4.3) and the rod is dropping from the top of the core, the axial node with the peak power remains the same (node 21 where node 24 is at the top of the core).

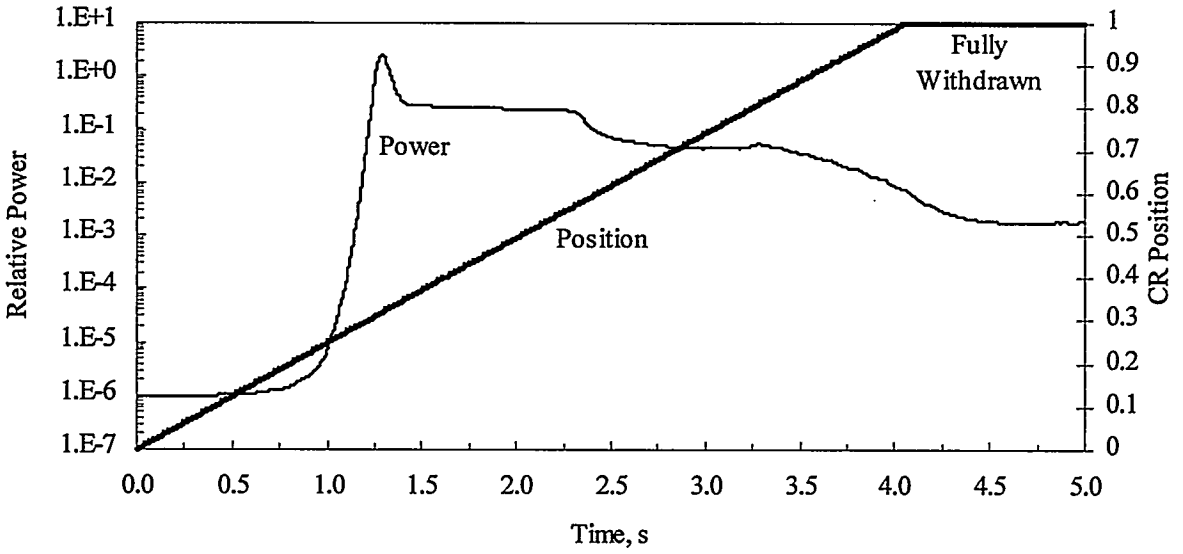

Figure 4.4 Power and Rod Position During RDA (Medium Burnup Case)

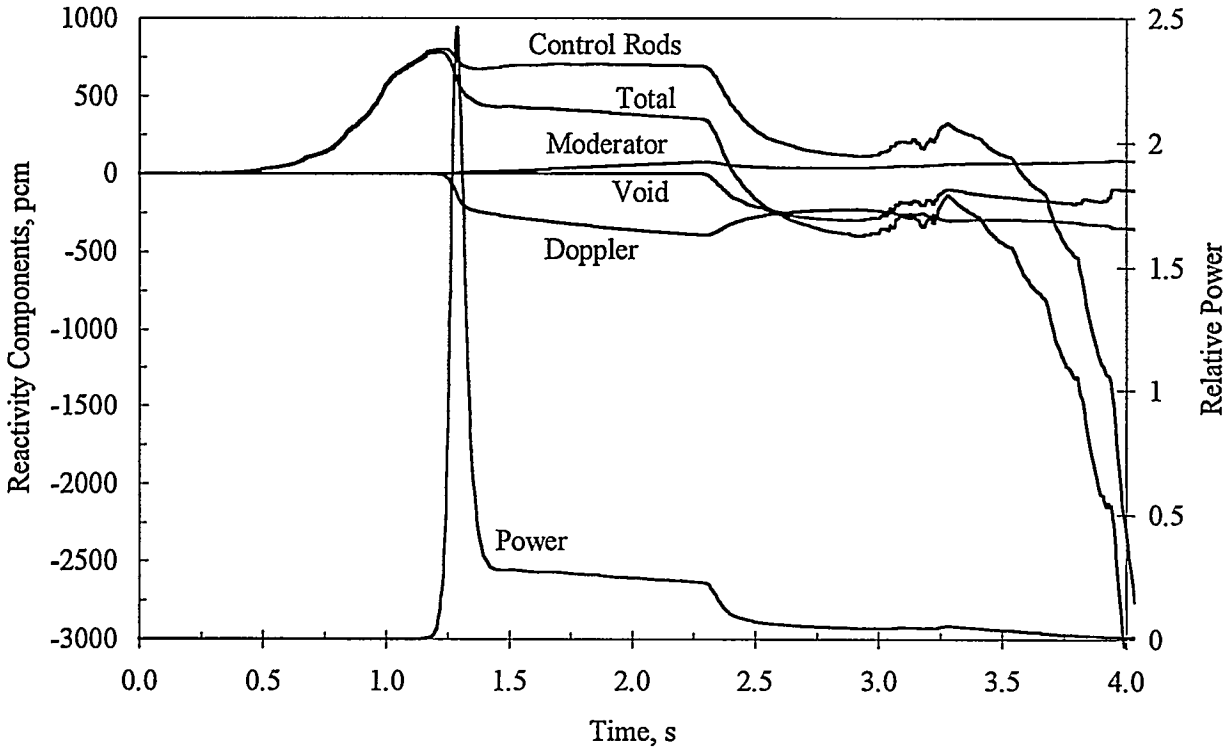

Figure 4.5 Reactivity Components During RDA (Medium Burnup Case)

1	3	2	3	8	6	5	7	15	14	11	15	34	32	27	38	81	129	90	118	236	375	269	361	769	1296	1129	1084	968	346
0	2	5	6	5	6	9	12	9	12	20	26	19	29	45	56	65	77	167	189	184	223	472	537	543	711	1268	1133	611	175
0	2	5	5	5	5	11	10	10	12	23	22	22	26	58	71	53	82	137	209	167	231	371	545	399	608	880	918	451	127
1	3	2	3	7	9	5	7	14	19	12	15	29	42	29	40	91	93	79	110	254	269	205	263	567	582	407	362	420	156
1	3	2	3	8	8	5	7	16	17	12	15	35	37	27	36	81	110	74	99	210	273	168	210	433	526	272	240	315	121
	2	4	6	4	6	9	12	9	13	21	27	21	27	40	49	54	69	132	141	132	141	268	280	254	243	373	305	176	54
	1	4	5	4	5	10	10	9	11	23	23	21	23	49	59	42	64	109	143	94	128	198	268	181	206	282	259	90	31
		1	3	6	8	5	6	12	16	11	13	25	34	24	31	66	66	55	67	137	130	98	119	224	204	157	83	53	
			2	6	6	4	6	14	14	10	12	28	29	20	26	55	72	45	55	110	135	78	86	162	172	87	34		
			1	2	4	7	10	8	10	17	21	15	20	29	34	36	40	76	77	69	73	117	111	81	54	41	23		
				1	2	7	8	8	8	18	18	17	18	35	41	30	41	61	76	48	61	87	93	38	19				
					1	3	5	9	12	8	10	19	25	16	20	42	42	31	34	65	63	49	38	22					
						1	2	8	9	6	8	18	19	12	15	32	38	22	24	46	50	20	11	10					
							1	2	5	7	9	9	10	15	18	17	19	26	27	22	15	10						
									1	2	3	2	3	5	6	4	5	9	9	6	4							

Figure 4.6 Radial Power Distribution During RDA (Medium Burnup Case)

Figure 4.7 shows the void fraction in a bundle being affected by the dropped rod. Although core average thermal-hydraulic parameters do not change significantly, the localized values change dramatically. The coolant temperature rises to saturation and then boiling begins. This is primarily the result of direct energy deposition although after approximately one second heat transfer across the cladding also becomes important. At the incipience of boiling, RAMONA-4B predicted flow oscillations and reversal in the hot channels. This in turn led to critical heat flux in a number of channels.

Boiling introduces negative reactivity and, therefore, could be important in mitigating the total enthalpy increase. In other situations, with little or no subcooling, boiling could begin very soon into the transient and reduce the power excursion and the immediate enthalpy increase. In these situations, there is a burden on the accuracy of the thermal hydraulics model being used. Although it is clear that a certain amount of energy deposition in the coolant leads to boiling, the timing could be important and current void generation models are based on experiments that do not mimic the dynamic conditions found during a RDA.

Fuel enthalpy (defined as the pellet radial average at any location in the core) is a key parameter in this study, as it is currently used in licensing calculations to determine the margin to the acceptance limit for the RDA (280 cal/g) and the condition for fuel failure (170 cal/g) for the purpose of calculating the radiological response. In the past, only the peak fuel enthalpy throughout the core has been of interest in licensing calculations, i.e., the maximum in both space and time. However, in the present study, it was of interest to understand the peak during the event as a function of the burnup of the fuel and that requires knowing the peak enthalpy in all the nodes in the region around the dropped rod. In the following, bundle enthalpy is discussed recognizing that if the results could be translated to an individual rod within a bundle, the fuel enthalpy would be higher. In order to know how much higher, one would have to do detailed calculations for the region surrounding the dropped rod. The hottest rod in a steady state might have a power 10-15 percent above the bundle average, but in the transient situation, the peaking could be quite higher.

Figure 4.8 shows the maximum fuel bundle enthalpy in three neutronic channels (fuel bundles) as a function of time. The maximum in time occurs in Channel 27 which is one of the bundles directly adjacent to the dropped control rod (CR #14 in Figure 4.1). Channel 56 is diagonally adjacent to Channel 27, and Channel 89 is one pitch removed from Channel 27. The predicted enthalpies are not at an axial plane but rather for an interval of 15.9 cm (6.3 in) corresponding to axial node 21 which is the node with maximum fission power. The legend shows the bundle burnup at the node in the bundle for which the enthalpy is a maximum. Reactor power history is also shown on the figure.

There are three distinct phases in the enthalpy plots: (1) prompt heatup due to the fission power excursion, (2) continuing fission power heatup, and (3) shutdown cool-off. Observation of the enthalpy curves indicates that in this particular calculation, the amount of prompt heatup is roughly equal to the fission power heatup. This results from the initial conditions, mainly from the high initial moderator subcooling which delays bulk boiling in the core--an important factor responsible for shutting down the fission reaction by introducing large negative void reactivity. A lower initial coolant subcooling would result in a lower maximum fuel enthalpy reached during the accident. Note that the separation of the fuel enthalpy increase into the first two phases may become particularly important if studies of fuel behavior in the future lead to acceptance criteria that are based on both the initial fuel enthalpy rise and the ultimate value.

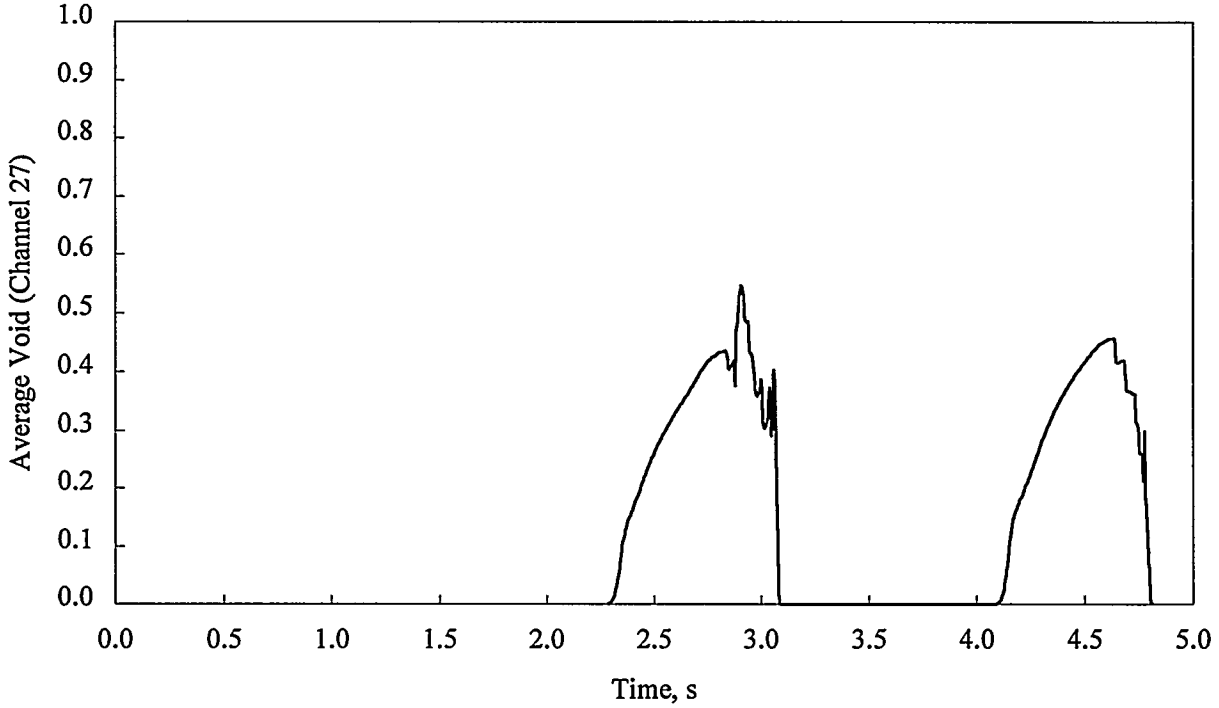

Figure 4.7 Void Fraction During RDA (Medium Burnup Case)

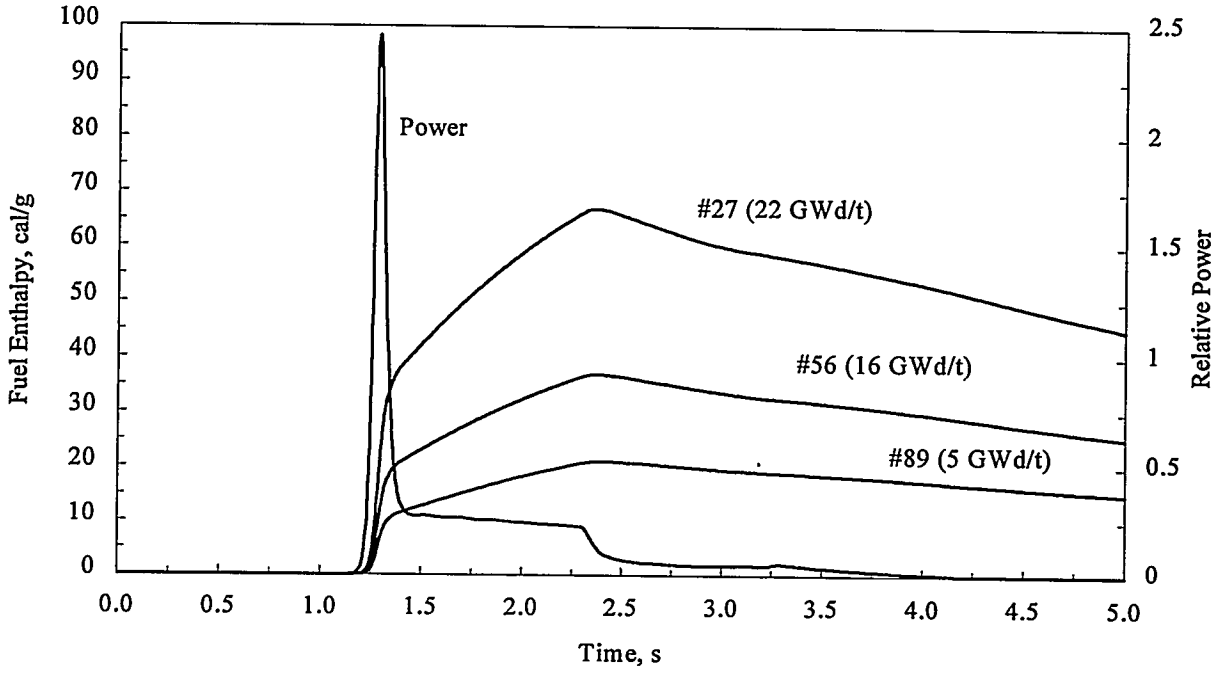

Figure 4.8 Maximum Fuel Bundle Enthalpy and Total Power During RDA (Medium Burnup Case)

The peak fuel enthalpy for this event (see Figure 4.8) is less than 70 cal/g which is considerably below the current values of interest from a licensing point of view. However, for this study, it was of interest to consider the fuel enthalpy as a function of burnup for a given RDA. Figure 4.9 shows enthalpy vs. burnup not just for the three bundles used to generate Figure 4.8 but rather for all of the 16 bundles (identified by number on the graph) of most interest surrounding the position of the dropped rod. The figure shows the orientation of these bundles relative to the dropped rod position of CR #14 which is between bundles 27 and 28. The figure also shows the location of other inserted control blades.

These results do not indicate a simple correlation between fuel enthalpy and burnup. Rather they suggest that for the given rod worth, the peak fuel enthalpy in a bundle is a complex function of factors, such as the distance of the bundle from that rod and the burnup of the fuel. In other cases for different control rod worths, the enthalpy in a given bundle could be higher or lower depending on the specific circumstances.

This conclusion is probably valid in spite of the fact that there are several other factors influencing Figure 4.9--namely, that (1) bundles 30 and 60 are on the core periphery and, therefore, the power surge is mitigated by the neutron leakage into the reflector and (2) the bundles with burnups of about 5 GWd/t have reactivities impacted by the burnout of gadolinium and, therefore, cannot be expected to have the same burnup dependence as bundles with higher burnups where gadolinium is no longer an important factor.

4.3.2 Results for a Pseudo High Burnup Core

The psuedo high burnup core, modeled as explained in Section 3.2, was used to calculate the effect of dropping CR #14 from a control rod pattern corresponding to 50 percent control rod density. The power versus time is shown in Figure 4.10 on a logarithmic scale. Reactivity components are shown in Figure 4.11. The behavior shown in these graphs is similar to that for the medium burnup case except that the peak power is higher. Although the fuel has a higher burnup in this case, the reactivity is not necessarily lower. More reactivity is designed into the fuel so that the reactor can continue to produce power at the higher burnup. Therefore, it is not surprising that results for the two burnup cases are similar.

The results for maximum fuel enthalpy versus burnup are shown in Figure 4.12 for the bundles surrounding the position of the dropped rod. Again, there is no clear correlation between burnup and enthalpy, and the conclusions discussed in Section 4.3.1 seem to apply here as well, i.e., that the enthalpy in any node depends on control rod worth, distance from the rod and also on burnup. In this figure and in Figure 4.9 for the medium burnup core, only the axial node with the peak enthalpy has been considered for a given bundle. Since the bundle burnup will be higher at nodes that are closer to the center of the core (see Figure 3.4), if these additional nodes were added to the plot, they would show points at higher burnup and lower fuel enthalpy relative to each of the points on the present plot. This would tend to create more points on the graph to the right and down from existing points. However, the nodes further away from the center (e.g., Nodes 23 and 24) would have lower enthalpy and lower burnup adding points to the left and down from the existing points. These additional axial points would, therefore, not be expected to reveal any trends and would not negate the possibility of relatively high enthalpy in a high burnup node if it were close to a high worth dropped control rod.

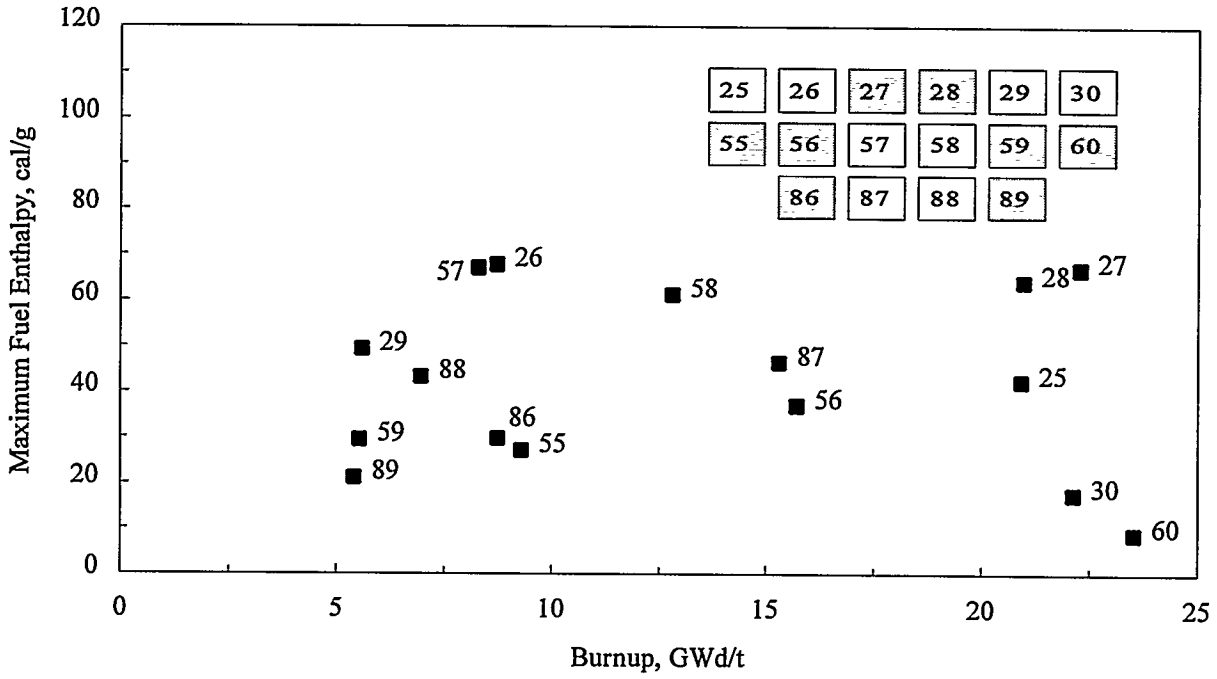

Figure 4.9 Maximum Fuel Bundle Enthalpy vs. Burnup (Medium Burnup Case)

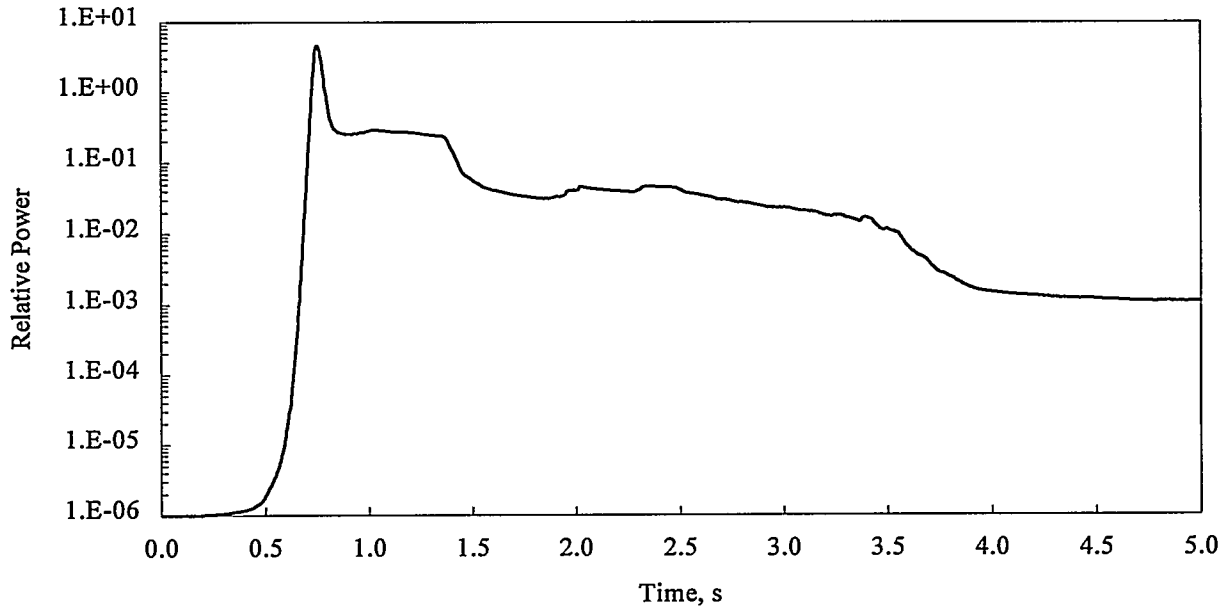

Figure 4.10 Power During RDA (Pseudo High Burnup Case)

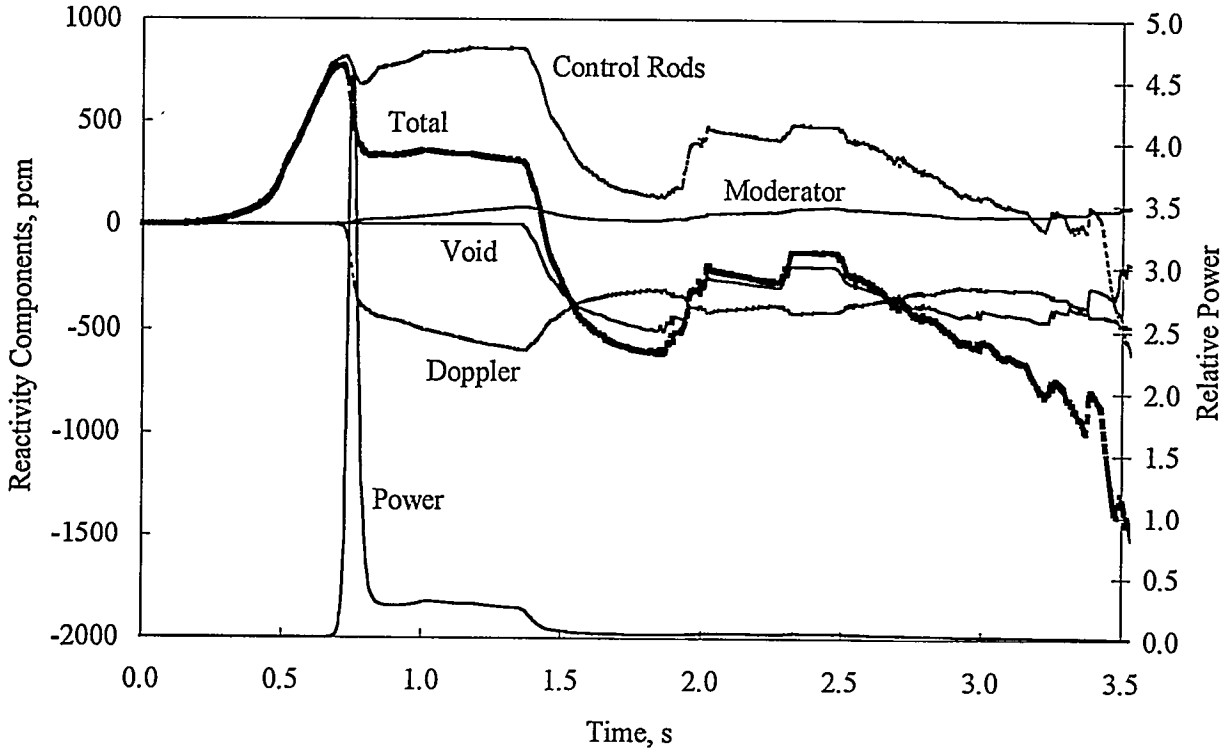

Figure 4.11 Reactivity Components During RDA (Pseudo High Burnup Case)

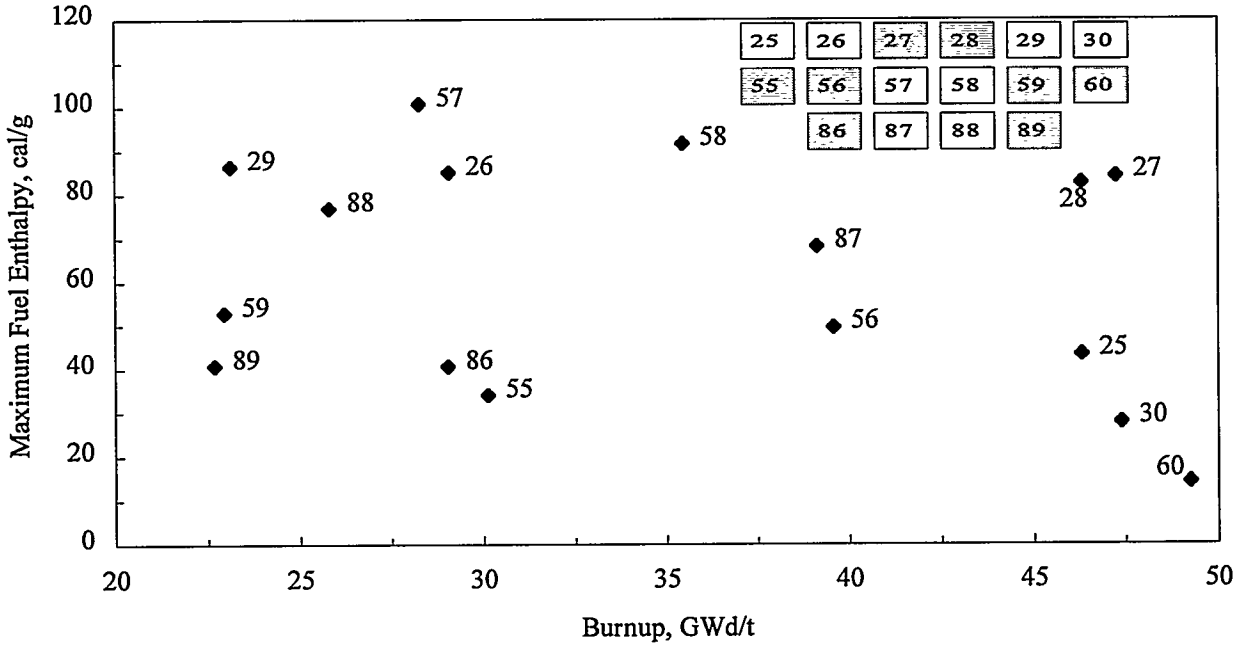

Figure 4.12 Maximum Fuel Bundle Enthalpy vs Burnup (Pseudo High Burnup Case)

4.4 Sources of Uncertainty in RDA Analysis

There are two general sources of uncertainty: (1) the methodology and (2) the assumptions used to define the reactor state. The methodology consists of the computer models and the values of the neutronic and thermal-hydraulic parameters that are used in those models. The validation of computer codes for application to the rod drop accident has always been a difficult matter. Since there have never been any rod drop accidents in a BWR, no data exist to directly assess the uncertainty in the calculated fuel enthalpy during a rod drop accident. Instead, the approach in the past has been to generally validate the computer codes and then to use a conservative approach to determine the margin to the acceptance limits for the rod drop accident. The conservative approach biases the assumptions used to define the reactor state so that the calculated peak fuel enthalpy is maximized. The assumption is made that the calculation uses so many conservative assumptions that the margin to the acceptance limits is reduced far more than if one did a best-estimate calculation and imposed a quantitative estimate of uncertainty to assure that there was still margin to the acceptance limits.

Although this has been a satisfactory practice, if a best-estimate approach is desired, it will be important to know the sources of uncertainties within the models and what impact these have on the uncertainty in fuel enthalpy in a given bundle.

To perform the general validation, data are used for related static and dynamic reactor conditions and comparisons are made with other calculations. For all operating plants, there are measurements available of the steady-state condition for criticality and the power distribution throughout the core. The computer code is used to calculate k_{eff} and the spatial power distribution, for a given reactor power, flow, and control rod pattern. This helps assure that the basic cross section library is capable of modeling both the fuel and control elements in the core and the important feedback due to fuel temperature and void. It also validates the neutronics and thermal-hydraulics modeling in the limit of steady-state operation.

Many plants also have measurements of key parameters during transients. Significant data exist for some plants where special tests were carried out. For example, turbine trip tests provide traces of pressure and reactor power both of which help validate the coupled neutronics and thermal-hydraulics modeling.

Comparisons of various transient and accident calculations with other codes also helps in the validation process. This is especially true when the comparisons are made based on standard benchmark problems which are calculated by many analysts.

This process can only go so far if the methodology is to be used in a best-estimate sense. One example of this is the need to consider void generation during the RDA and the fact that void generation models have not been validated under RDA conditions. This introduces an uncertainty into the analysis that is difficult to quantify without understanding void generation under rapid energy deposition conditions.

The validation process is complicated by the need to consider cores with high burnup fuel. Although existing methods should be able to extrapolate to modeling at high burnups, it is likely that this will increase the uncertainty in results. There are several implications of this in the basic reactor physics and thermal-hydraulic models which enter into the analysis.

The "rim" effect in high burnup fuel is of particular concern in the modeling. In general, the power distribution through a pellet is peaked at the surface due to self-shielding. This causes the plutonium concentration to grow at the surface [see, for example, (Lassmann, 1994)]. This effect accelerates with time so that the power and the plutonium distributions become highly peaked in a small region at the rim. The rim effect will impact the modeling of both reactor physics and heat conduction.

Reactor physics models that generate cross sections make assumptions about the temperature and power distributions across the pellet which might be in error due to the rim effect. Furthermore, because of the high concentration of plutonium at that location, it may be necessary to track more of the higher actinides than are currently modeled to reduce uncertainty.

The change in composition with burnup influences the thermal properties of the pellet, and data that are not generated for high burnup fuel will result in an increase in uncertainty. The rim effect introduces a spatial distribution of properties that may also become important. Furthermore, the uncertainty in calculations may increase if the heat conduction model does not account for the peaked spatial distribution of energy deposition in the pellet.

Two physics properties that may become more important with high burnup are the effect of the delayed neutron fraction (β) and moderator temperature feedback. The power excursion during an RDA is made worse when the delayed neutron fraction becomes smaller. The delayed neutron fraction decreases with burnup, and the ideal model would allow for the spatial distribution of β to account for the burnup throughout the core.

As discussed in Section 4.2, the moderator temperature feedback is positive when the moderator is relatively cold. The effect is made worse if there is significant subcooling. As with β, the effect becomes stronger with burnup, i.e., it is more important to model the effect for high burnup cores. This effect was somewhat quantified by redoing the calculation of the RDA discussed in Section 4.3.1 with no moderator temperature feedback. The results for power and fuel enthalpy are shown in Figure 4.13. As can be seen, the elimination of moderator temperature feedback had no significant effect on the initial power pulse and fuel enthalpy increase, but it did decrease the maximum enthalpy by approximately 5 cal/g. Since the moderator temperature reactivity coefficient is linear in the burnup range from 22 GWd/t (the burnup of the node with maximum enthalpy) to a high burnup value of 66 GWd/t, it is reasonable to expect that the effect may be on the order of three times as large or 15 cal/g for high burnup fuel.

Another source of uncertainty is the bundle power peaking factor which is used to calculate maximum fuel rod enthalpy given the maximum bundle average fuel enthalpy at a particular axial position. It is necessary to use this factor because most transient analysis is done with computer codes that model the bundle as an homogenized region. The peaking factor is an approximate means of accounting for the power distribution in the bundle and is straightforward to use to find the maximum fuel enthalpy in the bundle. However, this peaking factor is usually taken from a single-bundle calculation which assumes an infinite array of uncontrolled bundles. This does not account for the actual environment of the bundle which might sustain a large power gradient due to the particular control rod pattern. In order to account for the local power peaking more accurately, it is necessary to either use a transient calculation with a model for fuel rod power reconstruction or a supplemental steady-state calculation of rod by rod power that accounts for the actual reactor configuration during the RDA.

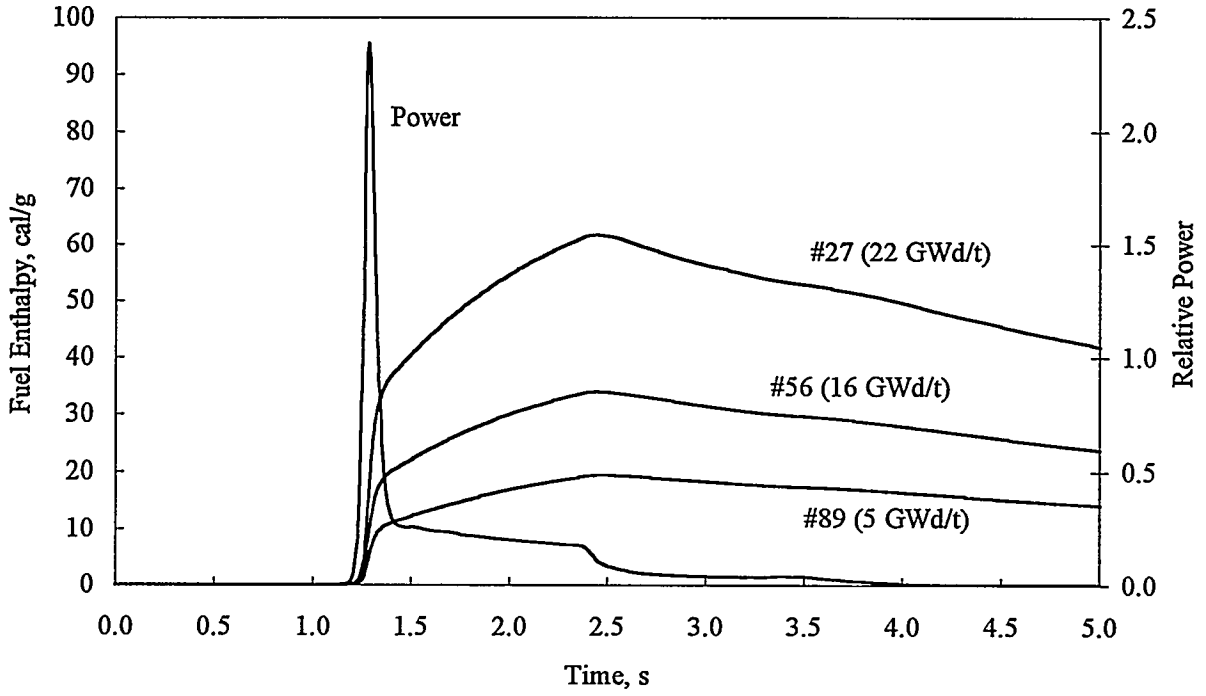

Figure 4.13 Maximum Fuel Bundle Enthalpy During RDA Without Moderator Temperature Feedback

4.5 Analysis of Thermal-Hydraulic Transients

4.5.1 MSIV Closure

Some of the reactor parameters applicable to both the MSIV closure calculation (Transient 1) and that for the recirculation flow controller failure (Transient 2) are given in Table 4.3. The first of these transients started from full power by the closing of all main steam isolation valves (MSIVs) over four seconds. All control rods were assumed to be out of the reactor at the start of the event. The initial power distribution is given in Figures 3.5 and 3.6. The reactor scram setpoint was 120 percent of full power with a 0.2-second delay. Typical values for pressure setpoints for the safety/relief valves (S/RVs) were used in the calculation.

Table 4.3 Reactor model parameters for thermal-hydraulic transients

Parameter/Condition	Value/Description Transient 1/Transient 2 where applicable
Fuel bundle maximum burnup	30
Reactor power relative to rated power of 3.29 GW	100%/68%
Control rod insertion pattern	All rods out
Delayed neutron fraction	0.006
Xenon inventory	Equilibrium
Reactor trip setpoint	120% of rated power with 0.2 s delay
Scram insertion speed	1.2 m/s (3.9 ft/s)
System pressure	6.92 MPa
Liquid temperature (core inlet)	269 °C
Core flow rate relative to rated flow	100%/50%
S/RV Setpoints	7.72, 7.79, 7.86, 8.72 MPa

The MSIV closure event was calculated for the first five seconds following the beginning of MSIV closure. By the end of this period, the reactor was scrammed, and the reactor core was cooling down. The power surge caused by the positive reactivity insertion due to void collapse was terminated by scram.

System pressure and core void are shown in Figure 4.14. As pressure increased and reached the level of the S/RV setpoints, the S/RVs started to open (timing for Banks 1 and 3 are shown in Figure 4.14), thus reversing the system pressure surge. The pressure rise was responsible for a decrease in void

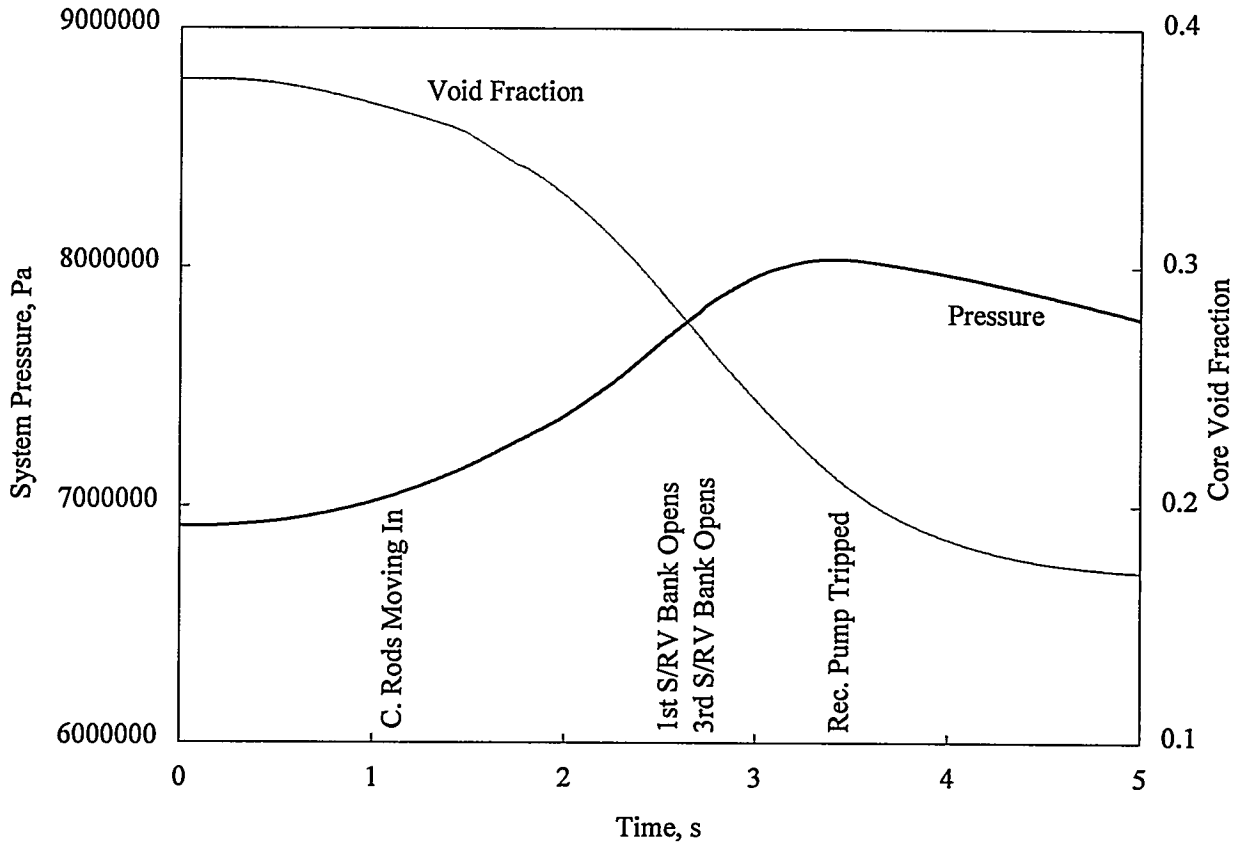

Figure 4.14 Pressure and Void Fraction During MSIV Closure Event

fraction and an increase in fission power shown in Figure 4.15[1]. The void fraction kept decreasing even after the pressure surge was over. This occurred because of a decrease in thermal power (also shown in Figure 4.15). The thermal power, or energy deposition into the coolant, decreased due to scram, and a consequent drop in vapor generation kept the void fraction decreasing. The control rods started to move into the core at approximately 1.1 seconds, and the recirculation pump was tripped on a high system pressure signal at about 3.4 seconds.

Figure 4.16 gives results for the major reactivity feedback components. The transient is driven by two competing feedbacks: void and scram. The moderator and fuel temperature (Doppler) effects are of minor importance in this transient.

Figure 4.17 shows the predicted history of maximum fuel enthalpy in the core. The peak increase over the duration of the transient is approximately 13 cal/g. The graph also shows the maximum and average fuel temperature during the transient.

4.5.2 Failure of a Recirculation Flow Controller

As noted in Section 2.2, it is the failure of the recirculation flow controller which is the thermal-hydraulic transient with the potential for causing the highest fuel enthalpy increase. This transient is caused by an increase in flow rate leading to the insertion of positive void reactivity when the void fraction decreases. In order to have a large increase in flow rate, it is necessary to start this transient from a flow rate considerably below nominal conditions. The starting point was, therefore, at a power 68 percent of nominal and a flow 50 percent of nominal. All control rods were out of the core simulating moving down a line of constant control rod density on the power-flow map. Although there are various procedures defining the reactor trip setpoint on high neutron flux depending on the flow rate, the setpoint in the present calculation was a conservative 120 percent of rated power. Reactor parameters are given in Table 4.3.

The core inlet flow history emulated the transient conditions found in a BWR/4 FSAR. One of the two recirculation pumps was ramped to rated level from the initial conditions. At the end of the transient (2 s), the core inlet flow rate was around 70 percent of nominal. Figure 4.18 shows core flow rate and fission power histories during the predicted transient.

As the core inlet flow increased, the core void fraction dropped leading to positive void reactivity insertion, which can be seen in Figure 4.19, showing the reactivity components during the event. At 1.35 seconds, negative reactivity due to scram, together with the negative fuel temperature reactivity, starts to reverse the power surge. The effect of control rod insertion on the shape of the axial power distribution can be seen in Figure 4.20, which shows the axial power distribution at time zero and at the time of maximum total reactor power.

Figure 4.21 shows that the maximum fuel enthalpy during this transient starts at 47.5 cal/g and increases approximately 3 cal/g. However, the initial enthalpy at the location where it is a maximum during the transient was approximately 20 percent less than the maximum (see Figure 4.20). Hence,

[1]Note that the oscillations in power are caused in part by the use of a nodal model to represent scram. Cusping occurs when the control rods cross a nodal boundary and the effect of the rods instantaneously affects the entire node.

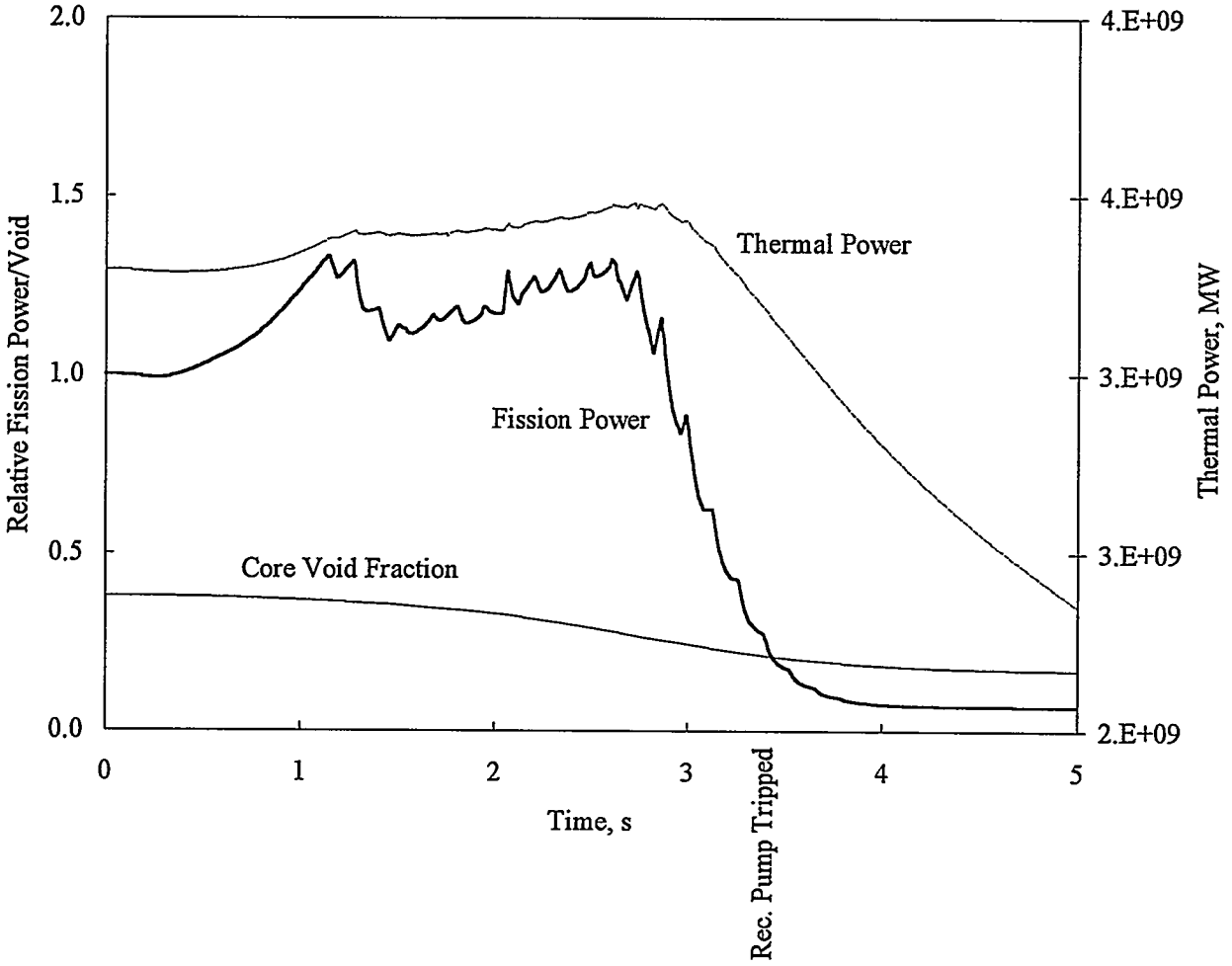

Figure 4.15 Power and Void Fraction During MSIV Closure Event

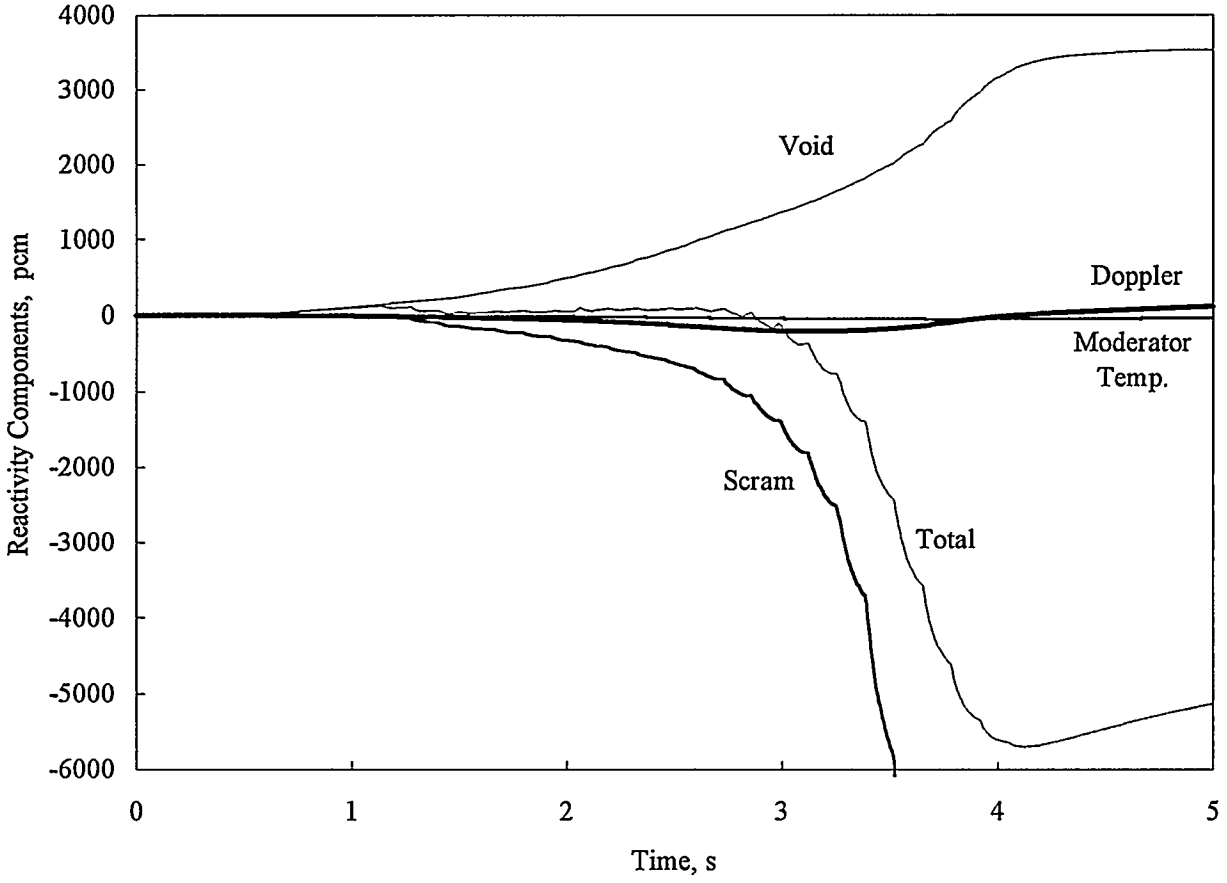

Figure 4.16 Reactivity Components During MSIV Closure Event

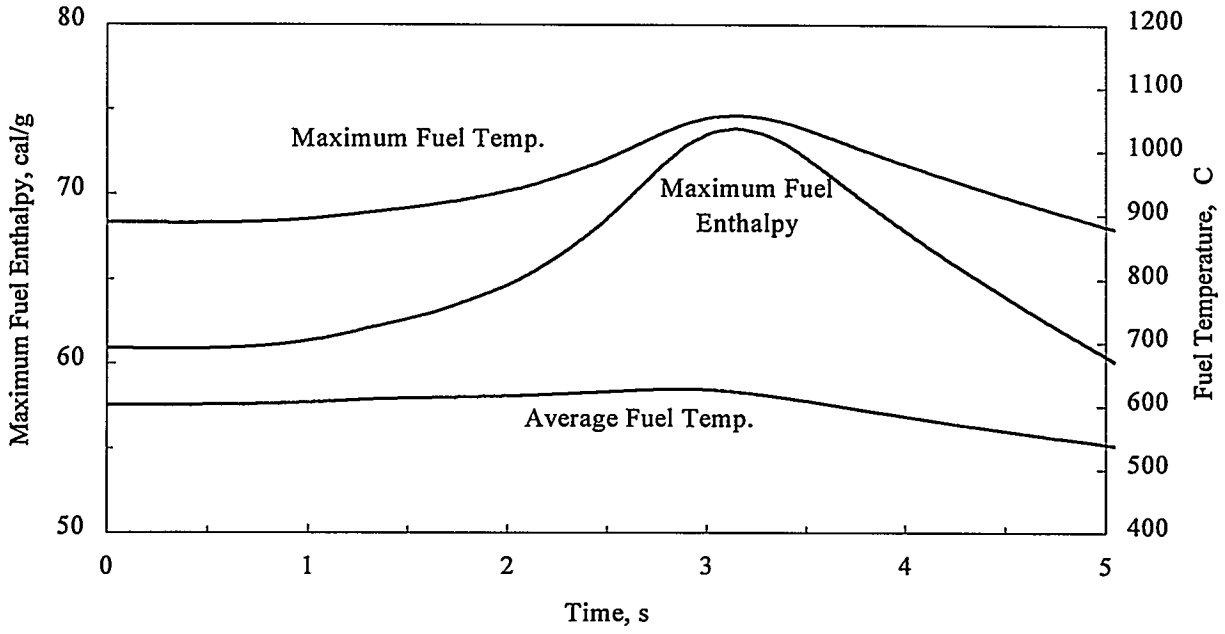

Figure 4.17 Fuel Enthalpy and Temperature During MSIV Closure Event

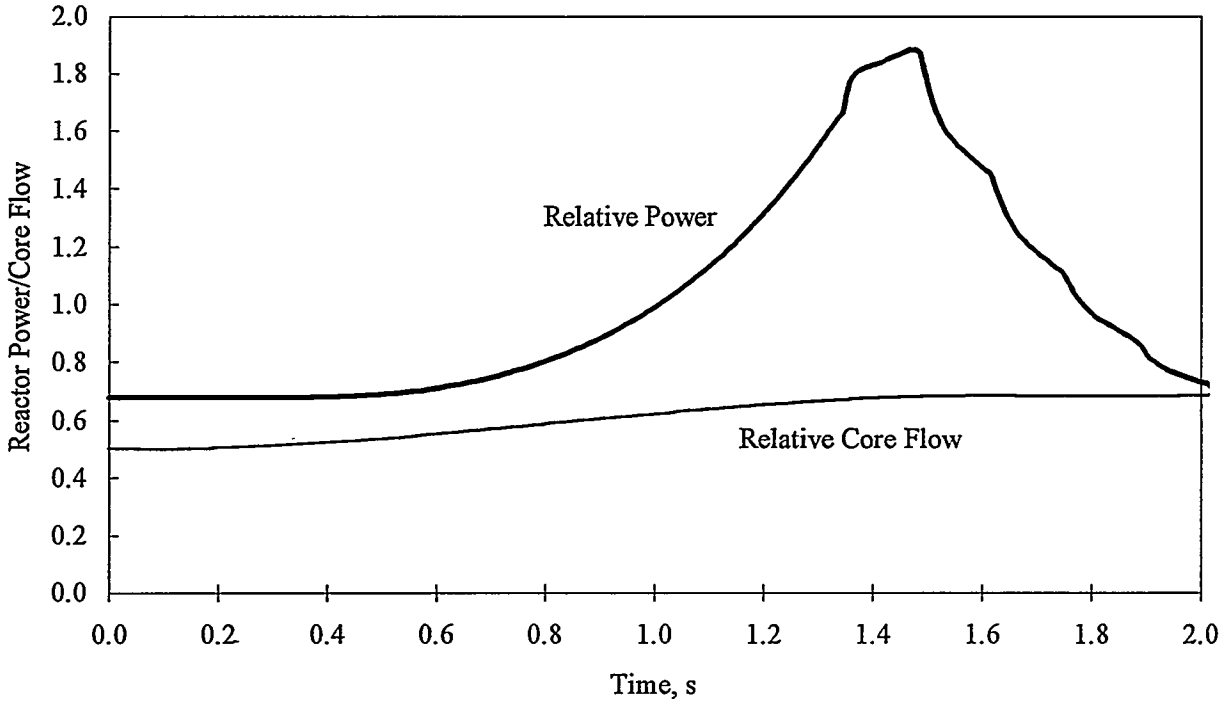

Figure 4.18 Power and Flow During Recirculation Flow Transient

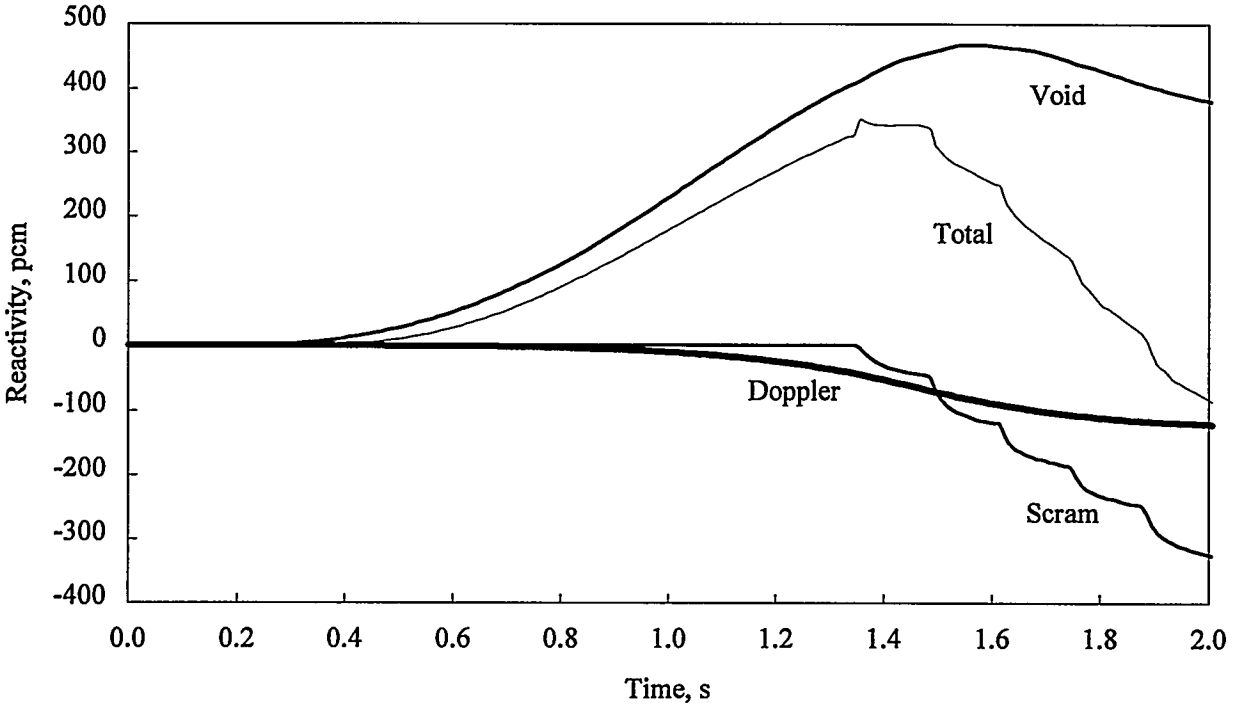

Figure 4.19 Reactivity Components During Recirculation Flow Transient

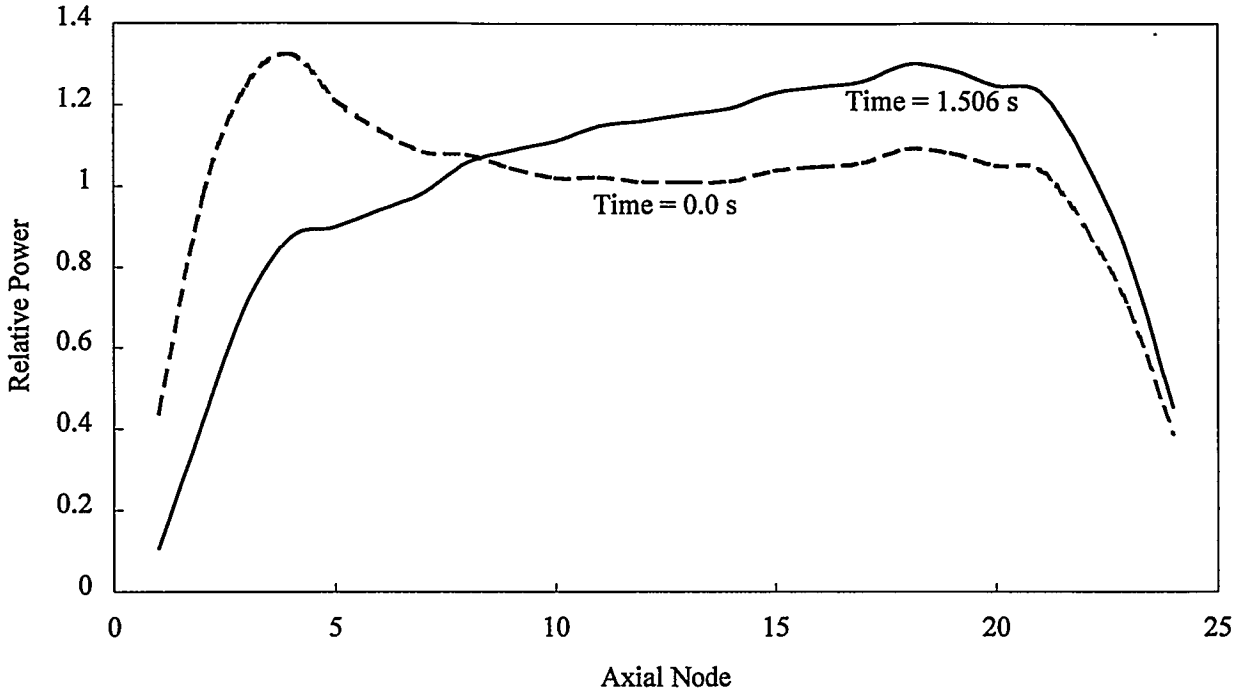

Figure 4.20 Axial Power Distribution During Recirculation Flow Transient

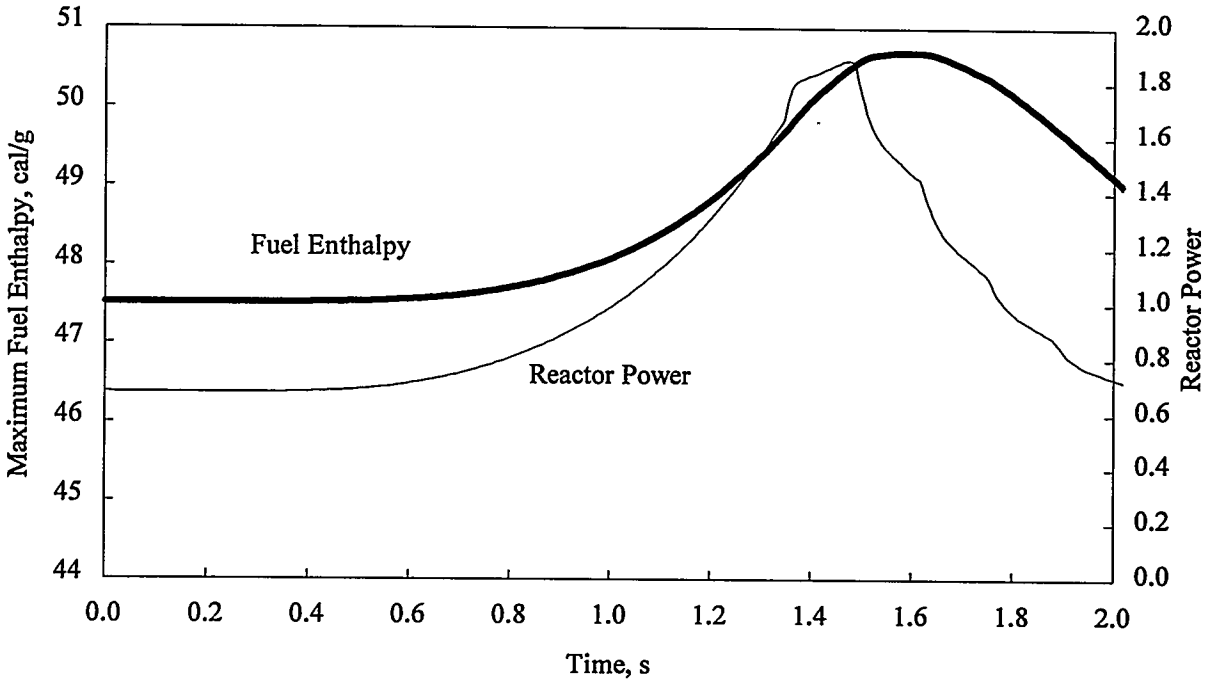

Figure 4.21 Power and Enthalpy During Recirculation Flow Transient

the increase in fuel enthalpy during this event is approximately 12 cal/g, which is comparable to that found for the overpressurization transient considered in Section 4.5.1.

5 REFERENCES

Ahlin, A., M. Edenium, and H. Häggblom, "CASMO: A Fuel Assembly Burnup Program," AE-RF-76-4158 (Rev Ed), Studsvik Energiteknik AB, June 1978.

Belblidia, L. A. and J. M. Kallfelz, "Analyses of Reactivity Insertion Accidents in the Mühleberg Boiling Water Reactor," STARS-Bericht Nr. 8A, Paul Sherrer Institute, January 1993.

Cheng, H. S. and D. J. Diamond, "Analyzing the Rod Drop Accident in a Boiling Water Reactor," *Nucl. Tech., 56*, January 1982.

Diamond, D.J., et al., "Reactivity Accidents with the Potential for Catastrophic Fuel Damage," *Nuclear Safety, 31*, 3, July-September 1990.

Diamond, D.J., et al., "Probability and Consequences of Rapid Boron Dilution in a PWR," NUREG/CR-5819, Brookhaven National Laboratory, June 1992.

Grandi, G.M., and L. Moberg, "Application of the Three-Dimensional BWR Simulator RAMONA-3 to Reactivity Initiated Events," Proceedings of the 1994 Topical Meeting on Advances in Reactor Physics, Knoxville, Tennessee, American Nuclear Society, April 1994.

Lassmann, K., et al., "The Radial Distribution of Plutonium in High Burnup UO_2 Fuels," *J. of Nuclear Materials, 208,* p. 223, 1994.

Nourbakhsh, H. P., and Z. Cheng, "Potential for Boron Dilution During Small Break LOCAs in PWRs (A Scoping Analysis)," Technical Report W-6156, Brookhaven National Laboratory, February 15, 1995.

Paone, C.J., "Banked Position Withdrawal Sequence," NEDO-21231, General Electric Co., January 1977.

U.S. Nuclear Regulatory Commission, "Reactivity Insertion Transient and Accident Limits for High Burnup Fuel," NRC Information Notice 94-64, August 31, 1994.

U.S. Nuclear Regulatory Commission, "Reactivity Insertion Transient and Accident Limits for High Burnup Fuel," NRC Information Notice 94-64, Supplement 1, April 6, 1995.

Valtonen, K., and D. J. Diamond, "Evaluation of ATWS Events in the Advanced Boiling Water Reactor," Technical Evaluation Report, Brookhaven National Laboratory, July 1992.

Wulff, W., et al., "A Description and Assessment of RAMONA-3B MOD.0 Cycle 4: A Computer Code with Three-Dimensional Neutron Kinetics for BWR System Transients," NUREG/CR-3664, Brookhaven National Laboratory, January 1984.

APPENDIX A

GENERATION OF NEUTRONIC DATA

A.1 Methodology

The lattice physics code CPM (Ahlin, 1975) was used to generate the neutronic fuel assembly data required for the representation of high burnup fuel in RAMONA-4B. The code can handle pressurized and boiling water reactor (PWR/BWR) fuel assemblies with cylindrical fuel rods of varying compositions arranged in a square array. For a BWR, it is capable of modeling the cruciform control rods, water gaps, and burnable absorbers. The code uses a 69-group microscopic cross section library that is based on ENDF-B/III.

The code first calculates effective cross sections for the resonance absorbers based on tabulated resonance integrals. The spatial screening effects of each fuel pin are taken into account by calculating appropriate Dancoff-factors. A 69-group infinite medium spectrum is then calculated, using the method of collision probabilities, for each type of representative fuel pin. The resulting micro-group fluxes are used to condense the cross sections to the (seven) group structure used in the 2-dimensional assembly calculations.

The depletion of burnable absorbers (gadolinium, Gd) is modeled by depletion dependent effective Gd cross sections provided by an auxiliary code MICBURN (Edenius, 1975). For a BWR assembly, the effects of the wide and narrow water gaps are included in the condensed spectra by weighting the cylindricalized assembly group fluxes with specific weight factors. The collapsed spectra and averaged cross sections constitute the basis for the 2-dimensional collision probability calculations providing a detailed spatial and energy dependent flux distribution in the fuel assembly. This flux distribution, in turn, is used to generate the assembly averaged 2-group cross sections for each specific case.

The 2-group cross sections generated by CPM form a point-wise discrete data set representing the effects of different variables. The primary factor determining the number of CPM calculations is the cross section model in the RAMONA-4B code. The formalism used in RAMONA-4B to represent the cross section types is given as

$$\Sigma = \Sigma(E, V, \alpha, T_f, T_m, f)$$

where E is exposure, V is void history, α is instantaneous void fraction, T_m and T_f are moderator and fuel temperatures, and f represents the presence or absence of control rods. Table A.1 lists each of the 2-group cross sections used in RAMONA-4B and the respective independent variables.

Depletion calculations with different void fractions, where void history and instantaneous void fractions are the same, and with nominal reference moderator and fuel temperatures for the composition without control rod presents are called the "nominal grid." The "off-nominal" assembly calculations are run at fewer times accounting for the presence of control rod, changes in moderator and fuel temperature, and changes in void contents with and without control rods present.

Table A.1 Two-Group Cross Section Representation

Energy Group	Cross Section	Independent Variables*
Fast, Group 1	Diffusion Coeff., D_1	E, V, f, α, T_m
	Removal, Σ_{r1}	E, V, f, α, T_m, T_f
	Total, Σ_{t1}	E, V, f, α, T_m, T_f
	Fission, $\nu\Sigma_1$	E, V, f, α, T_m, T_f
Thermal, Group 2	Diffusion Coeff., D_2	E, V, f, α, T_m
	Absorption, Σ_{a2}	E, V, f, α, T_m
	Fission, $\nu\Sigma_2$	E, V, f, α, T_m

*Legend:E	Exposure (MWd/t)
V	Void Fraction History
α	Instantaneous Void Fraction
T_m	Moderator Temperature
T_f	Doppler Fuel Temperature
f	Control Rod

RAMONA-4B has some restriction on the maximum number of compositions that may be explicitly represented, and hence, the number of fuel types used is limited. There exists an exposure and void history distribution which makes every node in the core unique. Therefore, a procedure is required to lump some nodes together in a single composition so that the fuel type limit is not exceeded.

The code BLEND (Eisenhart, 1980) combines 2-group cross section data with bundle exposure and void history distributions to optimally model a reactor core. The code reduces the number of compositions needed to represent the core by combining similar nodes into a common composition. It automatically selects arbitrary nodes that contain similar cross sections to be represented by the same composition regardless of their position in the reactor.

BLEND reduces the initial large number of compositions through an optimization procedure until a specified number of distinct compositions remain. Nodes belonging to a given composition are then averaged to produce the final cross section set for that composition.

A.2 Data Generation

The BWR/4 core used in this study was modeled using 8x8 fuel bundle designs from an operating reactor. The core contained nine different bundle types. These bundles were grouped into three different types, depending on their neutronic characteristics, to reduce the number of calculations. The bundles contain fuel rods with different U-235 enrichment and certain rods also contain gadolinia which acts as a burnable absorber. The different fuel types contained different U-235 loadings. Because the gadolinia loading was axially dependent, additional fuel bundle types had to be defined to distinguish the axial location. The fuel bundles were classified into a total of five fuel types depending on the

amount of Gd present. Figure A.1 indicates the axial variation of the Gd distribution in the different fuel types.

To obtain a high burnup core, the radial enrichment distribution in each bundle was increased linearly with the restriction that the maximum pin enrichment must be no more than the licensing limit of 5 percent. The extrapolation to higher enrichment was done to assure that the high burnup core would have the same residual reactivity as the medium burnup core at the end of the fuel cycle. The medium burnup core corresponding to the end-of-cycle at an operating plant had a maximum fuel bundle burnup of approximately 30 GWd/t while the high burnup core was meant to represent a core with a maximum of 60 GWd/t. The high burnup bundles were also expected to have a local power distribution similar to existing designs. The resulting peak fuel pin power factors were not unreasonable and were in the range of 1.5-1.6.

The fuel assembly calculations done with CPM to generate the high burnup data were done at the statepoints given in Table A.2. Depletion calculations were done on a grid that is finer than that used for the parametric calculations, e.g., for different fuel temperatures. For each fuel type and each void history, the table shows a total of 34 depletion statepoints and 49 additional parametric statepoint calculations. For the three different void histories and five fuel bundle types, it was necessary to calculate cross sections at a total of 1245 statepoints.

The cross sections for each fuel assembly types represent a discrete set of points with a number of dependencies. In the reactor core, each node as represented by the RAMONA-4B model is unique due to the variations in fuel type, exposure, and void history. This represents an enormous modeling problem which is reduced by BLEND through an optimization algorithm.

The input required for BLEND is the discrete cross section set as a function of many variables and the nodal exposure and void history data. The latter was obtained by extrapolating a 3-dimensional exposure distribution available from an operating plant. The actual end-of-cycle exposure and void history was extrapolated to simulate the expected distributions at the end of a cycle with high burnup fuel. The extrapolation routine used a simple parametric power-law dependency to generate the nodal distributions. The single parameter was selected after iterating between BLEND and RAMONA-4B by generating different composition sets and the corresponding steady-state power distribution. Only when the steady-state power distribution looked reasonable was the iteration concluded.

A.3 References

Ahlin, A. and M. Edenius, "The Collision Probability Module, EPRI-CPM," Advanced Recycle Methodology Program System Documentation, Part II, Chapter 6, Electric Power Research Institute, November 1975.

Edenius, M. and A. Ahlin, "MICBURN, Microscopic Burnup in Gadolinia Fuel Pins," Advanced Recycle Methodology Program System Documentation, Part II, Chapter 7, Electric Power Research Institute, November 1975.

Eisenhart, L. D. and D. J. Diamond, "Automatic Generation of Cross Section Input for BWR Spatial Dynamics Calculations," BNL-NUREG-28796, Brookhaven National Laboratory, November 1980.

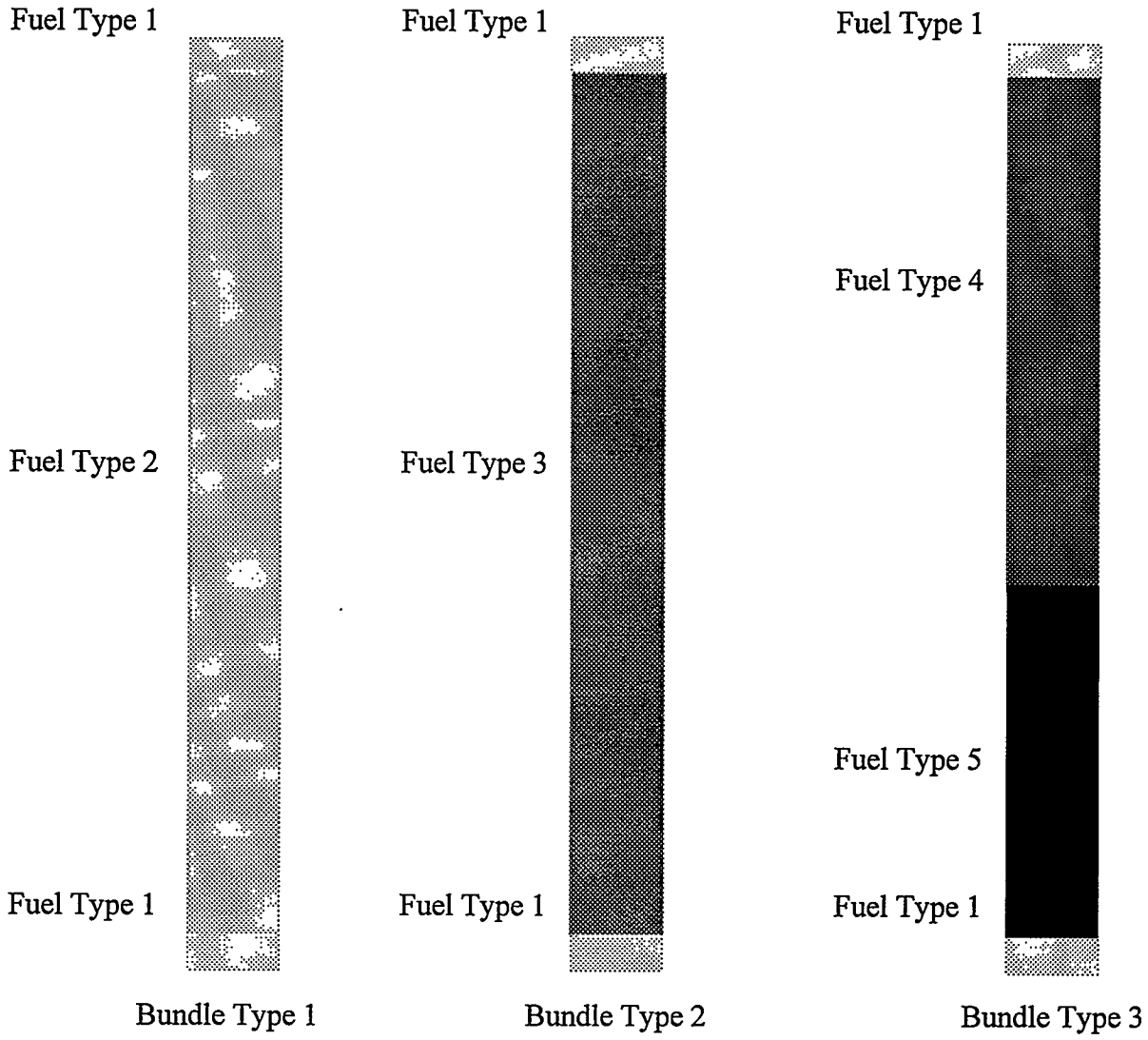

Description of Fuel Types:

Type 1 - No gadolinia, natural uranium fuel
Type 2 - 6 fuel pins with 2% Gd_2O_3
Type 3 - 7 fuel pins with 4% Gd_2O_3
Type 4 - 3 fuel pins with 2% and 4 fuel pins with 4% Gd_2O_3
Type 5 - 7 fuel pins with 4% Gd_2O_3

Figure A.1 Assembly and Fuel Types by Axial Zones

Table A.2 Statepoints for Fuel Assembly Calculations

Exposure MWd/t	Depletion Step*	Parametric Calculations**	Exposure MWd/t	Depletion Step*	Parametric Calculations**
0	x	x	12,500	x	
500	x		15,000	x	
1,000	x		17,500	x	
1,500	x		20,000	x	x
2,000	x		22,500	x	
2,500	x		25,000	x	
3,000	x		27,500	x	
3,500	x		30,000	x	x
4,000	x		32,500	x	
4,500	x		35,000	x	
5,000	x	x	40,000	x	
5,500	x		45,000	x	
6,000	x		50,000	x	x
6,500	x		55,000	x	
7,000	x		60,000	x	
7,500	x		65,000	x	
10,000	x	x	70,000	x	x

* Depletion calculations are done for three different void fractions which becomes the void history. They are done at a reference moderator and fuel temperature with control rods absent.

** Parametric calculations are done at another fuel temperature, another moderator temperature, with a control rod present, and at two other void fractions both with and without a control rod present (i.e., a total of seven parametric calculations). This is done for each of the sets of depletion calculations.

APPENDIX B

CONTROL ROD WORTH FROM A SPECIFIC ROD PATTERN

B.1 Analysis

The calculations performed for this study assumed that initially there was a checkerboard insertion pattern (50 percent control density as shown in Figure 4.1) for the control rods. One of the initially inserted control rods was then assumed to drop out of the core. Since this study was of limited scope, no attempt was made to consider the dozens of patterns that might be present in an operating reactor if the rod drop accident were to occur. The dropped rod worth can only be determined realistically by looking at each of these patterns. For licensing purposes, the possibility of a single error in withdrawing rods should also be considered.

Although no attempt was made to look at the multitude of possible patterns, it was of interest to consider one particular pattern because it looked similar to the checkerboard pattern actually used. This pattern was obtained by considering the steps delineated by the banked position withdrawal sequence (Paone, 1977). Figure B.1 shows a pattern possible when the control density is reduced just beyond 50 percent. The potential for a dropped rod occurs only for those rods where the drive mechanism has been removed, and the assumption is that the rod is stuck in the initial inserted position. From Figure B.1, that occurs in the regions with the rod fully withdrawn or withdrawn 12/48 of the distance of the core.

A RAMONA-4B calculation of rod worth was done assuming that CR #14 (see Figure 4.1) was initially stuck in the core and then dropped. The rod worth based on two static calculations was lower than that obtained using the checkerboard pattern because of the additional rods that are partially withdrawn in this case. It also is sufficiently low (less than the delayed neutron fraction) so that the RDA is expected to be inconsequential.

B.2 Reference

Paone, C. J., "Banked Position Withdrawal Sequence," NEDO-21231, General Electric Co., January 1977.

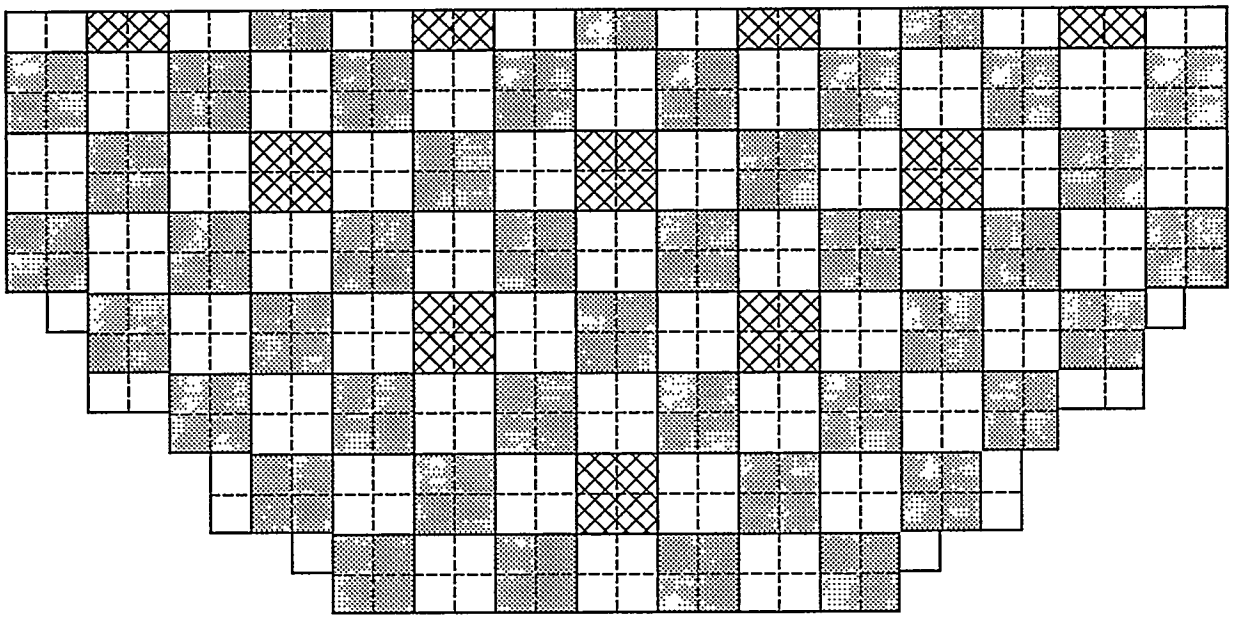

Unshaded core cells: control blade withdrawn 48 notches (fully)
Hatched core cells: control blade withdrawn 12 notches
Shaded core cells: control blade inserted

Figure B.1 Core Layout during Banked Position Withdrawal Sequence

APPENDIX C

EVALUATION OF THE MODERATOR TEMPERATURE REACTIVITY COEFFICIENT

C.1 Introduction

The moderator temperature coefficient (MTC) in a BWR at cold conditions is positive, i.e., an increase in temperature will increase reactivity. This well-known effect is generally not important because a BWR operates primarily at high temperatures, and at low temperatures, it is expected that the overall power coefficient is still negative. Nevertheless, the implication of a positive MTC for the rod drop accident (RDA) is that it could exacerbate the fuel enthalpy rise under certain conditions, and, therefore, it may have to be accounted for in RDA calculations.

In the following, the MTC is investigated for different conditions in order to quantify the effect for a typical fuel bundle design. The effect is broken into two components: one is due to the decrease in water density that occurs when temperature is increased, and the other is due to the increase in molecular motion that occurs. The latter is sometimes called the spectral effect because the increase in molecular motion increases the average energy of the thermal energy spectrum.

C.2 Calculational Model

The multigroup 2-dimensional transport theory code, CPM (Ahlin, 1975), was used to generate the fuel assembly data. The code can handle pressurized and boiling water reactor fuel assemblies with cylindrical fuel rods of varying compositions arranged in a square array. It is capable of representing the effects of the cruciform control rods between BWR bundles as well as water gaps and burnable absorbers. The code uses a 69-group microscopic cross section library that is based on ENDF-B/III.

The most common fuel lattice from a typical BWR/4 in its fifth fuel cycle was selected for calculational purposes. The bundle-average U-235 enrichment is 2.65 percent. Figure C.1 indicates the spatial distribution of the various pins. Pin 7 contains Gd as a burnable absorber. The burnup of Gd is calculated parametrically by the auxiliary code MICBURN (Edenius, 1975).

Three different base cases--corresponding to 0, 40, and 70 percent void history (void history V equal to void fraction α)--were calculated at exposure levels up to 50 GWd/t. The exposure steps were taken as suggested by the code, initially smaller than 0.5 GWd/t up to 7.5 GWd/t and then 2.5 GWd/t steps up to 50 GWd/t. The fuel temperature was 927.4 K, and the moderator temperatures were 600 K within the fuel channel and 560 K outside the fuel channel (in the bypass region).

In order to calculate the fuel bundle, MTC parametric cases were calculated for each of the void history calculations at exposures of 0, 5, 10, 20, 30, 40, and 50 GWd/t. The void fraction was set to zero and the fuel temperature to 373 K in all of the parametric cases. The MTC was then obtained by calculating the bundle k_{eff} with in-channel and bypass coolant at temperatures of 373 K and 293 K. In order to assess the effect of the density and spectral components, cases were also run relative to the case at 373 K. In one case, the density was changed to correspond to 293 K, and in another case, the temperature which determines scattering properties (but not the density) was changed to 293 K. These cases are summarized in Table C.1.

Bundle Array (45° Symmetry)	Pin	Enrichment (%)–Other Features
6 5 4 4 2 2 4 7 2 2 4 2 1 w 1 4 2 1 1 1 1 4 2 7 1 7 1 2 5 4 2 2 2 2 3 4	1	3.8
	2	3.0
	3	2.4
	4	2.0
	5	1.7
	6	1.3
	7	3.0 w/2.0 Gd
	w	Water hole

Figure C.1 Layout of an 8x8 Fuel Bundle

Table C.1 Cases Run to Assess Moderator Temperature Coefficient and Components

Case	Temperature corresponding to density	Temperature corresponding to spectral effect
a	373 K	373 K
b	293 K	293 K
c	373 K	293 K
d	293 K	373 K

C.3 Results

The results of the calculations of MTC are listed in Tables C.2, C.3, and C.4. In all cases with burnup, the MTC is positive and increases with exposure. The effect of void history is to reduce the magnitude of the MTC somewhat. The tables also list separately the components of the MTC due to changing only the density or only the spectral component. The results in Table C.3, corresponding to what would be close to the core average void history (40 percent), are shown graphically in Figure C.2.

Table C.2 MTC for an 8x8 Fuel Bundle with $V=\alpha=0\%$

Exposure GWd/t	MTC(total) pcm/K	MTC(density) pcm/K	MTC(spectral) pcm/K
0	-2.67	4.08	-6.98
5	12.09	4.84	6.97
10	12.65	4.51	7.86
20	17.63	4.71	12.61
30	24.83	5.33	19.12
40	32.98	6.11	26.38
50	39.72	6.73	32.39

Table C.3 MTC for an 8x8 Fuel Bundle with V=40%, α=0%

Exposure GWd/t	MTC(total) pcm/K	MTC(density) pcm/K	MTC(spectral) pcm/K
0	-2.67	4.09	-7.00
5	11.89	4.73	6.86
10	12.48	4.24	7.93
20	16.75	4.14	12.27
30	22.30	4.34	17.55
40	28.23	4.75	23.03
50	33.49	5.13	27.82

Table C.4 MTC for an 8x8 Fuel Bundle with V=70%, α=0%

Exposure GWd/t	MTC(total) pcm/K	MTC(density) pcm/K	MTC(spectral) pcm/K
0	-2.71	4.09	-7.05
5	11.39	4.60	6.50
10	12.23	3.96	7.95
20	15.64	3.56	11.74
30	19.65	3.40	15.84
40	23.63	3.40	19.78
50	27.09	3.45	23.13

C.4 References

Ahlin, A. and M. Edenius, "The Collision Probability Module, EPRI-CPM," Advanced Recycle Methodology Program System Documentation, Part II, Chapter 6, Electric Power Research Institute, November 1975.

Edenius, M. and A. Ahlin, "MICBURN, Microscopic Burnup in Gadolinia Fuel Pins," Advanced Recycle Methodology Program System Documentation, Part II, Chapter 6,Electric Power Research Institute, November 1975.

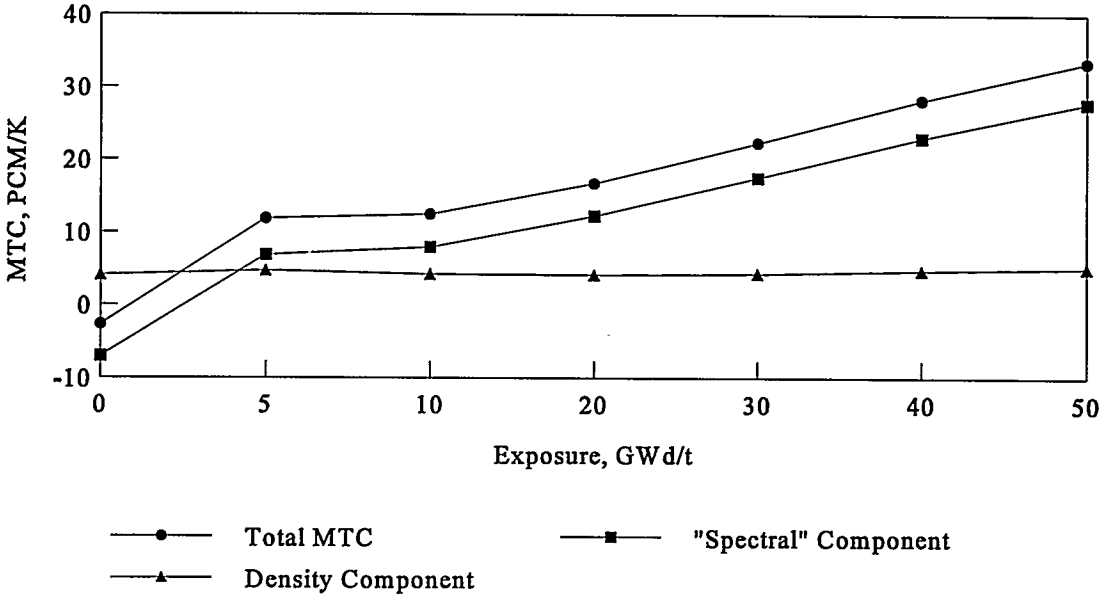

At Cold Conditions for 8x8 Lattice with Void History of 40%

Figure C.2 Fuel Bundle Moderator Temperature Coefficient

NRC FORM 335 (2-89) NRCM 1102, 3201, 3202

U.S. NUCLEAR REGULATORY COMMISSION

BIBLIOGRAPHIC DATA SHEET

(See instructions on the reverse)

1. REPORT NUMBER (Assigned by NRC. Add Vol., Supp., Rev., and Addendum Numbers, If any.)
NUREG/CR-6422
BNL-NUREG-52491

2. TITLE AND SUBTITLE
Power Excursion Analysis for High Burnup Cores

3. DATE REPORT PUBLISHED
MONTH: February
YEAR: 1996

4. FIN OR GRANT NUMBER
W6382

5. AUTHOR(S)
David J. Diamond, Lev Neymotin, Peter Kohut

6. TYPE OF REPORT

7. PERIOD COVERED *(Inclusive Dates)*

8. PERFORMING ORGANIZATION – NAME AND ADDRESS *(If NRC, provide Division, Office or Region, U.S. Nuclear Regulatory Commission, and mailing address; if contractor, provide name and mailing address.)*
Brookhaven National Laboratory
Upton, NY 11973-5000

9. SPONSORING ORGANIZATION – NAME AND ADDRESS *(If NRC, type "Same as above"; if contractor, provide NRC Division, Office or Region, U.S. Nuclear Regulatory Commission, and mailing address.)*
Division of Systems Technology
Office of Nuclear Regulatory Research
U.S. Nuclear Regulatory Commission
Washington, DC 20555-0001

10. SUPPLEMENTARY NOTES
D.D. Ebert, NRC Project Manager

11. ABSTRACT *(200 words or less)*
A study has been undertaken to determine the fuel enthalpy during a rod drop accident (RDA) and during two thermal-hydraulic transients in a boiling water reactor (BWR). The objective was to understand the consequences to high burnup fuel and the sources of uncertainty in the RDA calculations. The analysis was done with RAMONA-4B, a computer code that models the neutron kinetics throughout the core along with the thermal-hydraulics in the core, vessel, and steamline. The results showed that the calculated maximum fuel enthalpy in high burnup fuel will be affected by core design, initial conditions, and modeling assumptions. The important parameters in each of these categories are discussed in the report. An additional objective of this sutdy was to identify BWR and pressurized water reactor (PWR) transients in which there is significant energy deposition. This determined which BWR transients were to be calculated as part of this study and which might be calculated if analysis were to be done for PWRs.

12. KEY WORDS/DESCRIPTORS *(List words or phrases that will assist researchers in locating the report.)*
BWR Type Reactors-Excursions, BWR Type Reactors - Rod Drop Accidents, Fuel Elements - Enthalpy, PWR Type Reactors - Transients, BNL, Burnup, Computer Calculations, Computerized Simulation, Control Elements, Heat Transfer, Neutron Flux, R Codes, Reactor Accidents Reactor Kinetics, Thermodynamics

13. AVAILABILITY STATEMENT
Unlimited

14. SECURITY CLASSIFICATION
(This Page)
Unclassified
(This Report)
Unclassified

15. NUMBER OF PAGES

16. PRICE

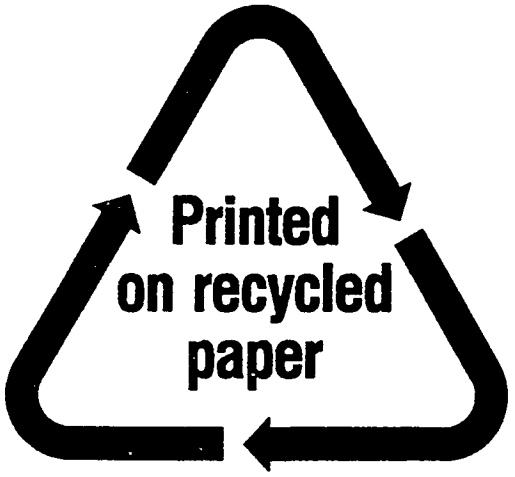

Federal Recycling Program